

Article

Rediscovery of Remarkably Rare Anaerobic Tentaculiferous Ciliate Genera *Legendrea* and *Dactylochlamys* (Ciliophora: Litostomatea)

Ondřej Pomahač ^{1,*}, Daniel Méndez-Sánchez ¹, Kateřina Poláková ¹, Michael Müller ², Michel-Marie Solito ³, William A. Bourland ¹ and Ivan Čepička ¹

¹ Department of Zoology, Faculty of Science, Charles University, Viničná 7, 128 00 Prague, Czech Republic

² Espental 11, D-93128 Regenstauf, Germany

³ Hydrobiology, Hautes-Fagnes Scientific Station, University of Liege, Rue de Botrange 137, 4950 Robertville, Belgium

* Correspondence: ondrej.pomahac@natur.cuni.cz

Simple Summary: Rare organisms represent a challenge for researchers in all fields of study in biology. In the realm of ciliatology, the genera *Dactylochlamys* and *Legendrea* are considered to be such cases. Very little information has accrued in over a century since their first descriptions; only a few published reports, online images or videos of rarely encountered individual specimens exist. *Dactylochlamys* and *Legendrea* are also morphologically remarkable for their likely independently evolved tentacle-like structures. Recently, the first molecular data were published for the species *L. loyezae*. In our study, we present more robust phylogenetic analysis based on three molecular markers of *Dactylochlamys pisciformis* and all of the three known *Legendrea* species, showing that they likely represent a new anaerobic lineage of ciliates. We first provide a detailed morphological characterization of both genera using modern microscopy and staining methods. We identify and discuss the bacterial (Syntrophaceae) and archaeal endosymbionts harbored by both genera based on 16S rRNA gene sequences. We also discovered that *Legendrea* preys on gastrotrichs, which is supported by molecular data and a unique video material documenting the feeding behavior of one *Legendrea* species. This study brings essential information needed to better understand the phylogeny, life strategies, and rarity of these organisms and emphasizes the importance of citizen science.



Citation: Pomahač, O.; Méndez-Sánchez, D.; Poláková, K.; Müller, M.; Solito, M.-M.; Bourland, W.A.; Čepička, I. Rediscovery of Remarkably Rare Anaerobic Tentaculiferous Ciliate Genera *Legendrea* and *Dactylochlamys* (Ciliophora: Litostomatea). *Biology* **2023**, *12*, 707. <https://doi.org/10.3390/biology12050707>

Academic Editors: Gaosen Zhang, Wasim Sajjad and Imran Khan

Received: 2 April 2023

Revised: 25 April 2023

Accepted: 10 May 2023

Published: 12 May 2023



Copyright: © 2023 by the authors. Licensee MDPI, Basel, Switzerland. This article is an open access article distributed under the terms and conditions of the Creative Commons Attribution (CC BY) license (<https://creativecommons.org/licenses/by/4.0/>).

Abstract: Free-living anaerobic ciliates are of considerable interest from an ecological and an evolutionary standpoint. Extraordinary tentacle-bearing predatory lineages have evolved independently several times within the phylum Ciliophora, including two rarely encountered anaerobic litostomatean genera, *Legendrea* and *Dactylochlamys*. In this study, we significantly extend the morphological and phylogenetic characterization of these two poorly known groups of predatory ciliates. We provide the first phylogenetic analysis of the monotypic genus *Dactylochlamys* and the three valid species of *Legendrea* based on the 18S rRNA gene and ITS-28S rRNA gene sequences. Prior to this study, neither group had been studied using silver impregnation methods. We provide the first protargol-stained material and also a unique video material including documentation, for the first time, of the hunting and feeding behavior of a *Legendrea* species. We briefly discuss the identity of methanogenic archaeal and bacterial endosymbionts of both genera based on 16S rRNA gene sequences, and the importance of citizen science for ciliatology from a historical and contemporary perspective.

Keywords: convergent evolution; infraciliature; methanogenic archaea; predatory ciliates; Spathidiidae; Syntrophaceae

1. Introduction

The phylum Ciliophora comprises a bewildering diversity of ciliated unicellular eukaryotes inhabiting virtually every biotope on Earth as both free-living organisms or

symbionts. Their enormous morphologic variety is matched by the many indispensable ecologic roles they play in terrestrial, freshwater, and marine microbial food webs. Eukaryovorous ciliates, an important guild of microorganisms, use various morphologic features for prey capture, and tentacles represent one of the most intriguing structures of this kind. Tentacles, as a feature of the ciliate cortex, have evolved several times in very distantly related lineages; e.g., the family Mesodiniidae and classes Phyllopharyngea and Litostomatea [1]. Ciliates of the class Litostomatea are known mainly as free-living aerobic eukaryovorous predators (subclasses Rhynchostomatia and Haptoria) or anaerobic endosymbionts inhabiting the guts of invertebrate and vertebrate hosts (subclass Trichostomatia) [2,3]. In addition to these varied lifestyles, litostomateans also exhibit some spectacularly diverse morphologic features, e.g., the skeletal plates of the endosymbiotic entodiniomorphids, the triple proboscises of *Teuthophrys* Chatton and Beauchamp, 1923, and the tentacles and papillae of *Actinobolina* Strand, 1928, *Dactylochlamys* Lauterborn, 1901, and *Legendrea* Fauré-Fremiet, 1908 [1,4,5].

The rarely encountered tentaculiferous ciliate genera *Legendrea* and *Dactylochlamys* have been assigned to the litostomatean family Spathidiidae based solely on their morphology [1,6]. The most distinctive features of *Legendrea* are tassel-like, ciliated, and extrusome-bearing tentacles which, in two species (*L. bellerophon* Penard, 1914 and *L. loyezae* Fauré-Fremiet, 1908), are highly extensible and have been assumed, but not proven, to be involved in prey capture [7]. On the other hand, the tentacles of *Dactylochlamys pisciformis* Lauterborn, 1901, the type and only species of the genus, are morphologically quite different from those of *Legendrea* and are more similar in appearance to those of *Actinobolina* and *Belonophrya* Andre, 1914, yet their functions remain unknown [4,5]. *Legendrea* and *Dactylochlamys* are vanishingly rare genera that may elude even the most widely traveled ciliatologists. To date, there have been only a few published reports, website images, and videos of *Legendrea* species and *Dactylochlamys* [5,8]. Thus, little information has accrued in over a century since their first descriptions.

In the genus *Legendrea*, three currently accepted species were originally described based on shared morphological features: *L. loyezae*, the type species, *L. bellerophon*, and *L. pespelicani* Penard, 1922. Four other species previously included in *Legendrea* by Penard (original combinations *L. crassa*, *L. interrupta*, *L. porculus*, and *L. simplex*) have been transferred to other genera in the order Spathidiida [9–11].

We present a phylogenetic analysis based on the ribosomal RNA cistron of *D. pisciformis* and all three *Legendrea* species, and also provide more detailed morphological characterization of *Legendrea* and *Dactylochlamys*, using protargol-impregnated specimens and scanning electron microscopy. We also present unique video material, including documentation of the feeding behavior of one *Legendrea* species, and discuss the putative bacterial (Syntrophaceae) and archaeal (*Methanobacterium* sp., *Methanocorpusculum* sp., and *Methanosaeta* sp.) endosymbionts harbored by both genera based on 16S rRNA gene sequences. Our results provide unique data essential to a better understanding of the phylogeny, life strategies, and rarity of these remarkable organisms.

2. Materials and Methods

2.1. Sampling

Sulfidic sediment samples from four freshwater localities in Belgium, the Czech Republic, Germany, and the USA were collected in 50 ml Falcon tubes. All populations in the original raw samples were kept in closed tubes for two to three weeks. Attempts to establish enriched and clonal cultures were unsuccessful.

The *Dactylochlamys pisciformis* population VB2A was found in the Venusbassin in Tiergarten Park in Berlin, Germany (52°30'52.5" N 13°22'14.2" E), and the MRATIN population in a eutrophic pond, Mratín, Czech Republic (50°11'58.7" N 14°33'17.2" E). The Czech populations of *Dactylochlamys* sp. (MOKOTP1Q), *Legendrea loyezae* (MOKOTL), and *L. ornata* (MOKOTP1) were found in a small permanent pond adjacent to the Vltava river in Prague (49°59'24.9" N 14°24'04.1" E). The US population of *L. ornata* (SAGEGLEN) came

from a small permanent eutrophic pond near Boise, Idaho (43°40′57.20″ N 116°15′15.44″ W), the Belgian population of *L. ornata* came from a freshwater garden pond in Tontelange, Province de Luxembourg (49°43′36.7″ N 5°48′32.1″ E), and the GTUB population from a garden mesocosm (see [12]). The Czech population of *L. pespelicani* (VLKOV) was found in a small permanent concrete-lined freshwater reservoir in the village of Vlkov (49°09′04.0″ N 14°43′22.4″ E).

2.2. Morphological Characterization

Living cells were hand-picked with glass micropipettes and studied at magnifications of 100–1000× with brightfield and differential interference contrast illumination, using an Olympus BX51 microscope equipped with an Olympus DP70 camera (Olympus Corp., Tokyo, Japan). Cells of VB2A were fixed with 4% (*v/v*) formalin and impregnated with protargol (Polysciences, Warrington, PA, USA) according to a modified Dieckmann's protocol [13–15]. *In vivo* measurements were made from photomicrographs of uncompressed, freely swimming cells, using calibrated software. Counts and measurements from protargol preparations were made at 1000× magnification. For scanning electron microscopy (SEM), cells were fixed for at least 30 min in 2.5% glutaraldehyde or in a 1:1 (*v/v*) solution of 5% glutaraldehyde and 2% osmium tetroxide, processed according to [14], and examined JSM-IT200 scanning electron microscope (JEOL LV, Peabody, MA, USA). Except as noted, morphological terminology and size classification follows [1,2,9,14]. For clarity, we refer to the cortical pellicular projections of *Dactylochlamys pisciformis* and the three species of *Legendrea* as “tentacles” and the trichocyst-bearing oral bulge structures of *L. pespelicani* as “papillae”.

2.3. DNA Extraction, Amplification, and Sequencing

In total, 3 cells from the VB2A population and single cells from the VLKOV, MOKOTL, MOKOTP1, and MOKOTP1Q populations were hand-picked with glass microcapillary pipettes, washed 5 times with distilled water, and added into 30 µL of DNA/RNA shield (Zymo Research, Irvine, CA, USA). The total DNA was isolated using the MasterPure™ Complete DNA and Purification Kit following the manufacturer's instructions. Three individuals of SAGEGLEN were picked for DNA extraction with a modified Chelex method [16].

The 18S rRNA gene (complete or almost complete) of SAGEGLEN and VLKOV was amplified using the primers EukA 5′-AACCTGGTTGATCCTGCCAGT-3′ and EukB 5′-TGATCCATCTGCAGGTTACCT-3′ [17], VB2A and MOKOTL were amplified with primers 82F 5′-GAAACTGCGAATGGCTC-3′ [18] and EukB, and the annealing temperature was 55 °C. MOKOTP1 was amplified with the primers 82F and the newly designed LEGR3 5′-TTCTCCTTCCTCTAGGTGATAAGG-3′, and the annealing temperature was 55 °C. An approximately 1200 bp long fragment of the ITS region and 5′ end of the 28S rRNA gene was amplified using the primers ITS-F 5′-GTAGGTGAACCTGCGGAAGGATCATT-3′ [19] and LO-R 5′-GCTATCCTGAGRGAACTTCG-3′ [20], and the annealing temperature was 54 °C. The 16S rRNA gene fragment (approx. 460 bp) of methanogenic Archaea was amplified using the primers Arc915F 5′-AGGAATTGGCGGGGAGCAC-3′ and ArcR1326 5′-TGTGTGCAAGGAGCAGGGAC-3′ [21,22], and the annealing temperature was 55 °C. The PCR products were purified using EXOSAP (Applied Biosystems, Waltham, MA, USA). Amplicons were directly sequenced on an ABI PRISM 3100 sequencer (Applied Biosystems). For taxonomic assignment of archaeal 16S rRNA gene fragments, the BLASTn algorithm was used (<https://blast.ncbi.nlm.nih.gov>, accessed on 29 March 2023).

The V4 variable region fragment of 16S rRNA gene (approx. 300 bp) from VLKOV and VB2A populations was amplified from extracted DNA (see above) for Illumina sequencing, using barcoded primers 515F 5′-GTGYCAGCMGCCGCGGTAA-3′ and 806R 5′-GGACTACNVGGGTWTCTAAT-3′ [23,24]. Paired-end (2 × 250 bp) Illumina amplicon sequencing (NovaSeq6000) and demultiplexing was performed at SEQme company (Dobříš, Czech Republic). Microbiome bioinformatic analyses were performed using the QIIME2

2022.8 platform with DADA2 plugin for denoising and chimera removal [25,26]. Amplicon sequence variants (ASVs) were taxonomically classified using the classify-sklearn naïve Bayes taxonomy classifier (via q2-feature-classifier plugin) [27] against the Silva 138 99% OTUs reference sequences of the 515F/806R region [28]. Dominant archaeal ASVs were identified as putative symbionts based on their relative frequency.

2.4. Phylogenetic Analyses

An alignment of 18S rRNA gene sequences included 167 taxa, comprising 135 litostomateans and 32 outgroup taxa representing Armophorea and CONThreeP [29]. Five litostomatean sequences are newly reported in this study and all other sequences were obtained from GenBank. The dataset of concatenated 18S-ITS-28S rRNA region sequences consisted of 168 taxa, including 6 newly determined sequences and 162 sequences (135 litostomateans and 32 outgroup taxa) obtained from GenBank. The sequences were aligned using the G-INS-i algorithm [30] on the MAFFT server (<https://mafft.cbrc.jp/alignment/software/>, accessed on 15 March 2023). The alignment was manually edited using AliView [31] to trim primer sequences. The length of the final 18S rRNA gene data set was 1825 positions and the concatenated data set comprised 3163 positions. Phylogenetic trees were constructed using the maximum likelihood (ML) and Bayesian inference (BI) methods. The best fit substitution model (GTR + I + Γ) was selected using Modeltest-NG [32,33]. ML analysis was performed in RAxML-NG [34] on the CIPRES portal (http://www.phylo.org/sub_sections/portal/, accessed on 15 March 2023) under the GTR + I + Γ substitution model. Statistical support was assessed using 1000 bootstrap pseudoreplicates and convergence assessed using weighted Robinson–Foulds distance. Bayesian analysis was performed using MrBayes 3.2.7 [35] on the CIPRES portal using the GTR + I + Γ substitution model. For the 18S rRNA gene alignment, Markov chain Monte Carlo (MCMC) analyses of four chains (three hot, one cold, temperature 0.2) and for the concatenated alignment six chains (five hot, one cold, temperature 0.1) were each run for 10 million generations, with a sampling frequency of 1000 generations. The first 25% of sampled trees were removed as burn-in. Convergence was assessed using RWTY [36]. Uncorrected p-distances were calculated using MEGA v10.2.6.

3. Results

3.1. Morphological Descriptions and Diagnoses

3.1.1. Dactylochlamys Pisciformis Lauterborn, 1901

Amended diagnosis based on [10,37,38] and current study. Moderately small-to-medium-sized spathidiid. Shape fusiform to clavate. Cortex rugose. One equatorial, globular to ellipsoidal macronucleus with one adjacent ellipsoidal micronucleus. Contractile vacuole subterminal. Somatic kineties follow left-hand spiral course. Long fine somatic cilia interspersed with very slender, rigid, tubular, capitate, retractile tentacles. Long filiform extrusome occupies lumen of each tentacle, and extends into cytoplasm when tentacles retract. Oral bulge truncate conical; base surrounded by short oblique pectinelles at anterior ends of somatic kineties.

Description based on VB2A (Figures 1 and 2; Table S1; Video S1). Size 85–110 × 25–35 μm in vivo ($n = 2$), about 60 × 18 μm after protargol impregnation, length:width ratio from 2.5–3.7 in vivo ($n = 2$) and about 3.6 in protargol preparations. Shape fusiform to clavate. Colorless. Single equatorial globular to ellipsoidal macronucleus about 8 × 6 μm with many small, scattered nucleoli in protargol preparations; single adjacent globular micronucleus about 2–3 μm across (Figure 2C). Contractile vacuole subterminal; excretory pores not observed (Figure 1A,B,F,G). Long, fine filiform extrusomes occupy lumen of tentacles; proximal ends extend into cytoplasm. Cortical granules not observed. Cytoplasm filled with refractive globules and large food vacuoles.

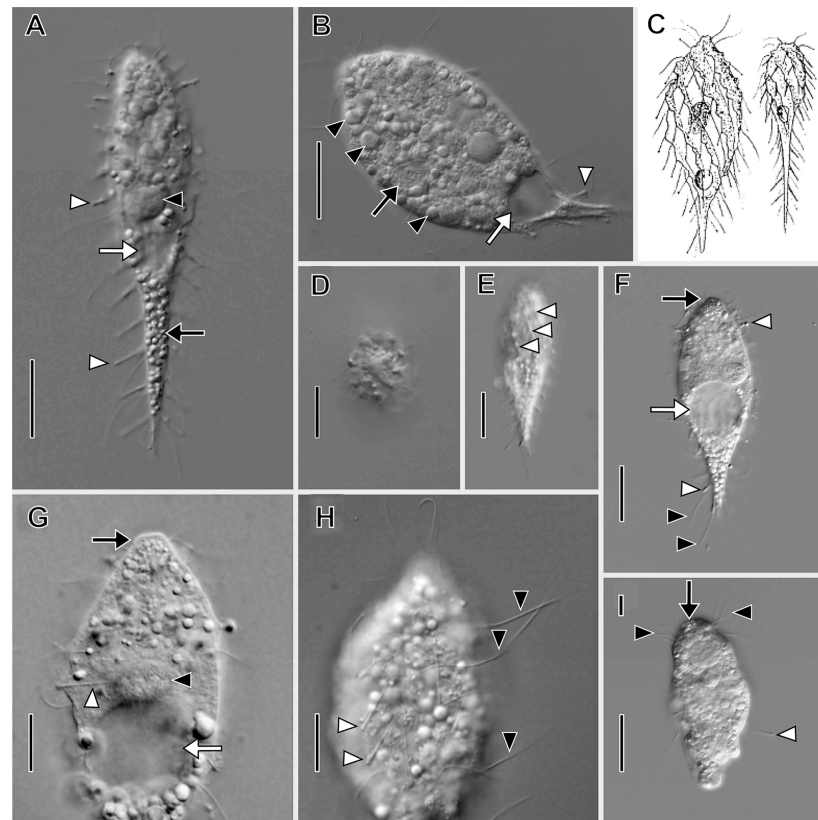


Figure 1. *Dactylochlamys pisciformis* from VB2A (A,B,E–H) and MRATIN (D) in vivo and a suctorian swarmer (I) in vivo. (A) Lateral view of a slender individual showing the inconspicuously capitate tentacles in varying states of extension (white arrowheads), the macronucleus (black arrowhead), the subterminal contractile vacuole (white arrow), and the refractile cytoplasmic globules (black arrow). (B) Lateral view of a broadly ellipsoidal individual showing the cytoplasmic globules (black arrowheads), the contractile vacuole (white arrow), and a retracted tentacle (white arrowhead). (C) Two variations in body shape, modified from Kahl presenting two morphotypes of *D. pisciformis*. (D) Circular cell shape viewed in optical cross section. (E) Lateral view showing the spiral cortical ridges (white arrowheads). (F) Lateral view showing capitate tentacles (white arrowheads), somatic cilia (black arrowheads), the contractile vacuole in diastole (white arrow), and the bluntly conical oral bulge (black arrow). (G) Lateral view, optical section showing extrusomes of a retracted tentacle extending into the cytoplasm (white arrowhead), the contractile vacuole in diastole (white arrow), the macronucleus (black arrowhead), and the oral bulge (black arrow). (H) Surface view showing the long, fine somatic cilia (black arrowheads) and the tentacles (white arrowheads). (I) Lateral view of suctorian swarmer form (similar to *Parapopdophrya solaris*) from the same sample as VB2A, showing an extended capitate tentacle (white arrowhead), the apical part of the cell superficially resembling the oral bulge of *Dactylochlamys* (black arrow), and the somatic cilia resembling the pectinelles of *Dactylochlamys* (black arrowheads); otherwise somatic cilia are absent unlike in *Dactylochlamys*. Scale bars: 20 μm (A–F,I), 10 μm (G,H).

About 10–12 ordinarily spaced somatic ciliary rows on slightly wavy left-hand spiraling ridges, short inclined ciliated pectinelle between anterior end of each somatic kinety and base of oral bulge, each pectinelle composed of three or four basal bodies. Kineties composed of monokinetids bearing long fine cilia (12–20 μm long), interspersed with tentacles. Tentacles very slender, tubular, retractile, about 15 μm long when extended, inconspicuously capitate when retracted, and each encloses an argyrophilic extrusome. Dorsal brush not observed.

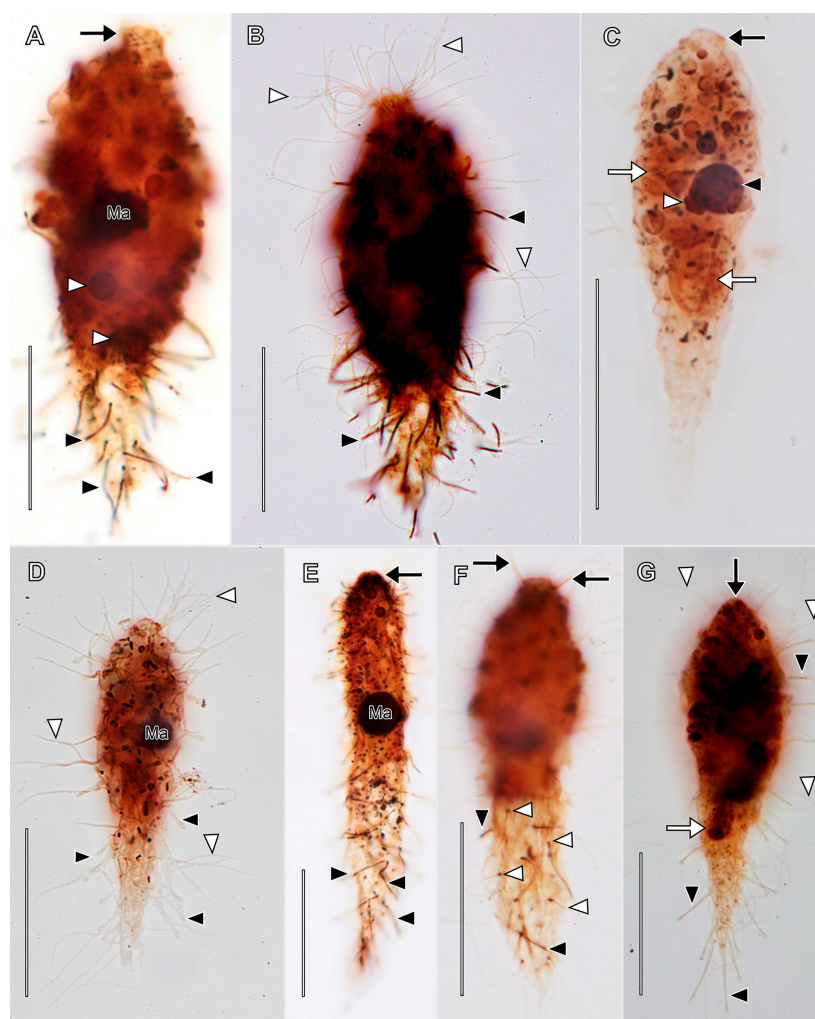


Figure 2. *Dactylochlamys pisciformis* from VB2A after protargol impregnation. (A) Optical section showing the oral bulge with left-hand-spiraling pectinelles comprising 3–4 basal bodies (black arrow), food vacuoles (white arrowheads), and the strongly impregnated (argyrophilic) tentacles (black arrowheads). (B) High-contrast view showing the long fine somatic cilia (white arrowheads) and the argyrophilic tentacles (black arrowheads). (C) Optical section showing the macronucleus with multiple small nucleoli (black arrowhead), the micronucleus (white arrowhead), the oral bulge (black arrow), and the food vacuoles (white arrow). (D) Cell showing long fine somatic cilia (white arrowheads) and inconspicuous unimpregnated tentacles (cf. A,B). (E) Slender individual showing the oral bulge (black arrow) and the tentacles (black arrowheads). (F) View showing the cilia of the oral bulge pectinelles (black arrows), the left-hand-spiraling somatic kineties (white arrowheads), and the tentacles (black arrowheads). (G) View showing the oral bulge (black arrow), a food vacuole with an ingested flagellate (white arrow), and the inconspicuous somatic cilia (white arrowheads) interspersed between tentacles (black arrowheads). Ma, macronucleus. Scale bars: 25 μm .

Oral bulge truncate conical, inconspicuous in vivo, about 2 μm high, 4 μm in diameter after protargol impregnation. Oral bulge extrusomes and cytopharyngeal basket not observed (Figure 2).

Based on our own observations, we accept Kahl's synonymization of *D. hystrix* Wetzel, 1928 with *D. pisciformis* [10]).

3.1.2. Legendrea Fauré-Fremiet, 1908

Amended diagnosis: Moderately small to large spathidiid. Tentacles, each with circumtentacular kinety and extrusome bundle, sometimes highly extensible, located on

dorsal and ventral margins or restricted to posterior one-half of cell. Sometimes with papillae in oral bulge. Inhabits anoxic or microoxic freshwater biotopes.

- *Legendrea loyezae* Fauré-Fremiet, 1908

Amended diagnosis (based on [7–10,39] and current study): With characters of genus. Size 70–132 × 62–85 μm in vivo. Shape broadly elliptical to almost spherical. Eccentric posterior contractile vacuole may appear as two vacuoles due to median cleft at posterior end when tentacles retracted. Up to 25 tentacles clustered posteriorly, never anterior to cell equator, trail limply behind swimming cells. Tentacles more or less tubular when retracted, distal ends mushroom-shaped when extended, often with an eccentric distal luminal vacuole, tentacular extrusome bundles 4.5–14 μm long, layer of smaller rod-shaped extrusomes beneath terminal cap of tentacles. Extended tentacles reach up to 6.5 times retracted length.

Description based on in vivo observations of MOKOTL ($n = 3$; Figure 3; Video S2): Size 85–102 × 55–102 in vivo, contractile. Shape broadly obovate to nearly globular, anterior end obliquely truncate; up to 25 flexible, trailing tentacles restricted to posterior one half of cell. Horseshoe-shaped macronucleus, micronuclei not observed. Contractile vacuole eccentrically located at posterior end, sometimes indented by median pellicular cleft when tentacles retracted, occupies entire posterior end in diastole (Figure 3C,D). Extrusomes in oral bulge, morphology not determined, tentacles with two types of extrusomes; one type curved, filiform, closely packed in central bundles at distal ends of tentacles (about 4.5 μm long); second type comprises layer beneath distal ends of tentacles, small (about 1.5 μm long), rod-shaped (Figure 3F,H,I). Ejected extrusomes not observed. Tentacles extensible, covered with granular layer near junction with cell body, distinct cortical ruffles (collar) not observed. Cytoplasm colorless but cells appear dark under low magnification. Cells packed with refractive globules, food vacuoles with ingested prey. Cells swim steadily at moderate pace and rotate rightward about long axis (Video S2).

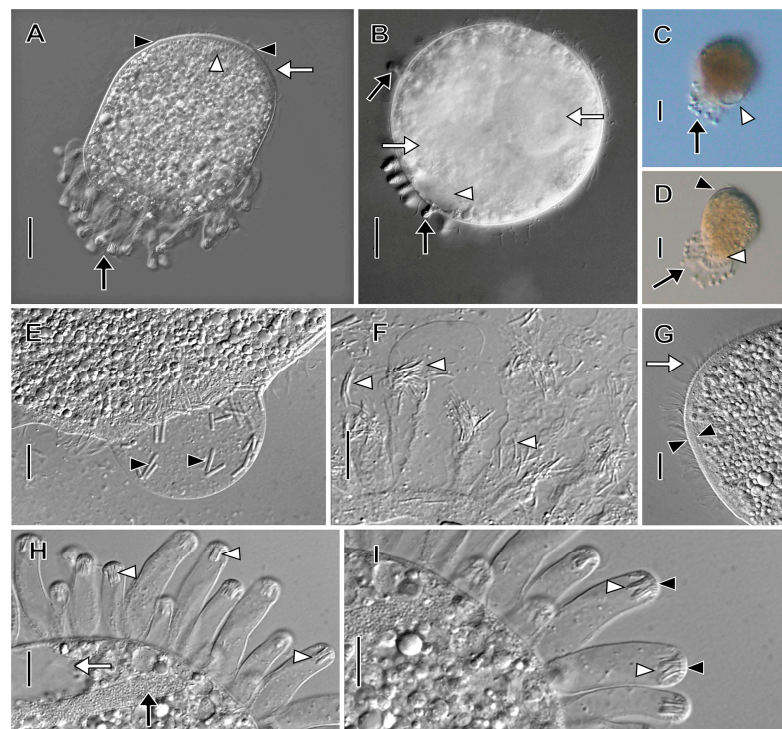


Figure 3. *Legendrea loyezae* from MOKOTL in vivo. (A) Lateral view of a swimming cell showing the oral bulge (between black arrowheads), the position of the dorsal brush (white arrow), the oral basket (white arrowhead), and trailing partially retracted tentacles (black arrow). (B) Lateral view of

a globular cell with retracted tentacles (black arrows) and ingested prey (white arrows) and showing the contractile vacuole (white arrowhead). (C) Lateral view showing the typical shape of a swimming cell and showing trailing retracted tentacles (black arrow) and the eccentric position of the contractile vacuole (white arrowhead). (D) Lateral view of the same specimen as A showing trailing tentacles (black arrow), the oral bulge (black arrowhead), and the contractile vacuole (white arrowhead), the same specimen as A. (E) Squashed cell showing prokaryotic endosymbionts (black arrowheads). (F) Squashed tentacles showing curved filiform tentacular extrusomes (white arrowheads). (G) The hyaline subcortical layer probably composed of mucocysts (between black arrowheads) and somatic cilia (white arrow). (H) Detail view of the posterior part of the cell showing tentacular extrusome bundles (white arrowheads), one end of the horseshoe-shaped macronucleus (black arrow), and the eccentrically located contractile vacuole (white arrow). (I) Detail of tentacles with approximately 5 μm long curved filiform extrusomes in bundles (white arrowhead) and a subcortical layer of much smaller (about 1.5 μm) rod-shaped extrusomes (black arrowheads). Scale bars: 20 μm (A–D), 10 μm (E–I).

Ciliature holotrichous, somatic cilia about 6 μm long in closely spaced longitudinal kineties; number of kineties not determined. Each tentacle with single circumferential subterminal kinety. Dorsal brush inconspicuous with approximately 3 μm long clavate cilia; number and morphology of brush rows not determined.

Oral bulge inconspicuous, less than 3 μm high, occupies two-thirds of anterior end, eccentric (i.e., displaced slightly ventrally). Oral basket inconspicuous.

Remark: We were unsuccessful in obtaining protargol preparations of *L. loyezae*.

- *Legendrea pespelicani* Penard, 1922

Amended diagnosis based on [9] and current study: With characters of genus. Size 180–210 \times 60–90 μm in vivo. Broadly spatulate in lateral view, laterally compressed. Oral bulge oblique, invariably contains one trichocyst-bearing papilla at either end, usually one or two papillae in between; thus, oral bulge outline moniliform or dumbbell-shaped when viewed anteriorly. Macronucleus filiform, very long, tortuous strand. About six stout, mushroom-shaped, ciliated, extrusome-bearing tentacles commence at or anterior to equator, distributed at irregular intervals on dorsal and ventral margins of cell, always one posterior polar tentacle. Tentacular extrusomes longer (about 25 μm) than those in tentacles of *L. ornata* or *L. loyezae*. Distinctly spathidiid somatic ciliary pattern. Circumtentacular kineties composed of many more dikinetids than in *L. ornata*. Ciliary rows interrupted by tentacles while deviating around tentacles in *L. ornata*. Tentacle extension characteristic for *L. loyezae* and *L. ornata* not observed.

Description based on VLKOV (Figures 4–6; Table S2; Videos S3–S5): Size about 180 \times 90 μm in vivo, about 165 \times 120 after protargol impregnation, length:width ratio 2 in vivo and 1.4 in protargol preparations. Shape broadly spatulate in lateral view, laterally compressed in vivo, less so in protargol preparations. Cells appear dark in vivo under low magnification. Single very long (up to 331 μm), tortuous, filiform macronucleus; nucleoli prominent in vivo (Figures 4I and 5). Five to nine scattered micronuclei (2.5–4 μm across). Extrusomes of one type, restricted to closely packed bundles in distal ends of tentacles and in oral bulge papillae, curved, filiform (about 25 \times 1 μm), do not impregnate with protargol. Contractile vacuole large, terminal, several subterminal excretory pores on right side (Figures 4F and 5C). Cortex flexible (Figure 4C). Cortical granules not observed. Cytoplasm filled with refractive globules (about 2–4 μm across) and large food vacuoles. Swims lazily (Videos S3–S5).

Somatic ciliation holotrichous, longitudinal ciliary rows interrupted by tentacles. Somatic cilia about 8 μm long, arranged in about 70 rows. Ciliary pattern distinctly spathidiid (i.e., right-side kineties curve dorsally to meet circumoral kinety, left kineties curve ventrally). Each tentacle with ciliated subcapital circumtentacular kinety composed of dikinetids (about 35 on average). Stout (about 8 μm high \times 10 μm across) mushroom-shaped tentacles (six on average) at irregular intervals on dorsal, ventral margins, invariably one tentacle at posterior pole (Figure 6A). Active tentacle extension not observed. Total

of 3 dorsal brush rows composed of dikinetids bearing 3.5 μm long clavate cilia, rows commence to left of dorsal oral bulge papilla; B1 and B2 extend posteriorly about 20% of cell length; B3 highly unusual, i.e., proximal part similar in morphology and length to B1 and B2 but posterior part composed of patchily distributed monokinetids and groups of dikinetids extending about 50% of cell length (Figure 6C,D,F).

Oral bulge oblique (about 40° to long axis of cell), convex anteriorly, long, narrow (about $80 \times 5 \mu\text{m}$). Circumoral kinety about 80 μm long, 5 μm wide between papillae, invariably encloses one extrusome-bearing papilla at dorsal and ventral end, usually one or two additional papillae between (two of nine individuals had only two oral bulge papillae: one dorsal, one ventral). Oral bulge papillae about 3.5 μm high \times 10 μm across. Outline of circumoral kinety moniliform or dumbbell-shaped when viewed anteriorly due to deviation around large papillae (Figure 5C,D,G). Large broadly conical oral basket extending nearly entire length of cell (Figure 5H).

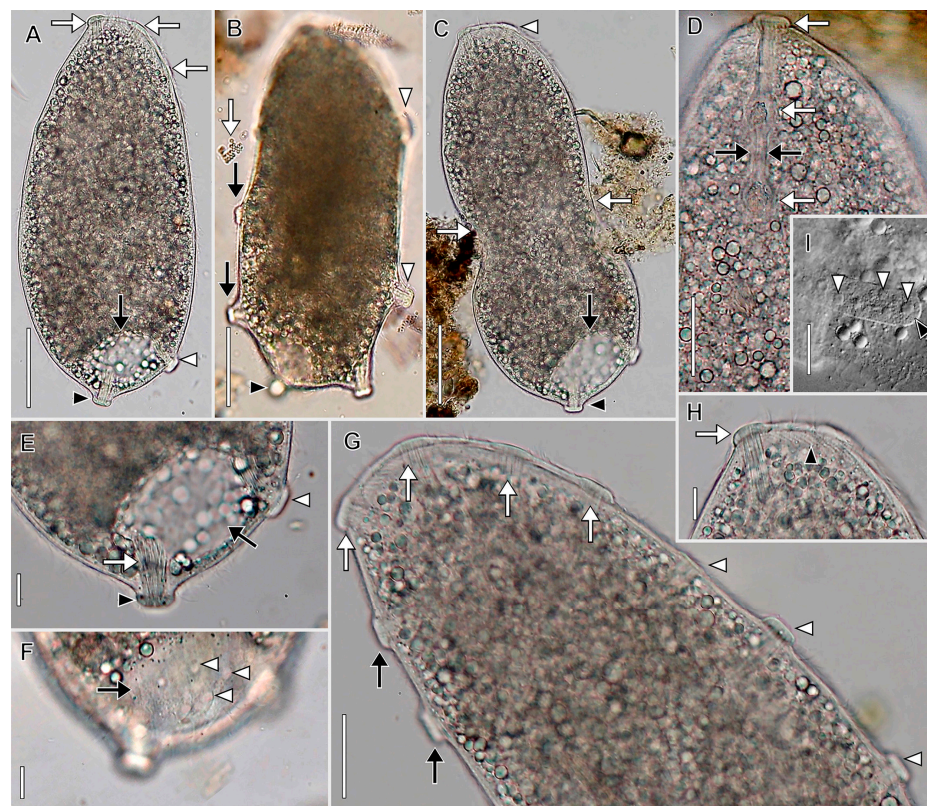


Figure 4. *Legendrea pespelicani* from VLKOV in vivo. (A) Right dorsolateral view showing three oral papillae (white arrows), the posterior terminal tentacle (black arrowhead), a ventral tentacle (white arrowhead), and the contractile vacuole (black arrow). (B) Lateral view showing dorsal tentacles (black arrows), ventral tentacles (white arrowheads), the terminal tentacle (black arrowhead), and a *Thiopedia rosea* platelet (white arrow). (C) Optical section showing the oral bulge (white arrowhead), flexible cortex (white arrows), the terminal tentacle (black arrowhead), and the contractile vacuole (black arrow). (D) Ventral view showing three oral papillae (white arrows) encompassed by the circumoral kinety (black arrows). (E) Detail of posterior end of the cell showing an extrusome bundle (white arrow) the terminal tentacle (black arrowhead), a ventral tentacle (white arrowhead), and the contractile vacuole (black arrow). (F) Surface view, the same cell as (E), showing excretory pores (white arrowheads) of the contractile vacuole (black arrow). (G) Optical section showing four oral papillae (white arrows), dorsal somatic tentacles (black arrows), and ventral tentacles (white arrowheads). (H) First oral papilla (white arrow) and somatic kinety furrows (black arrowhead). (I) The filiform macronucleus (black arrow) and nucleoli (white arrowheads). Scale bars: 50 μm (A–C), 25 μm (D,G), 10 μm (E,F,H).

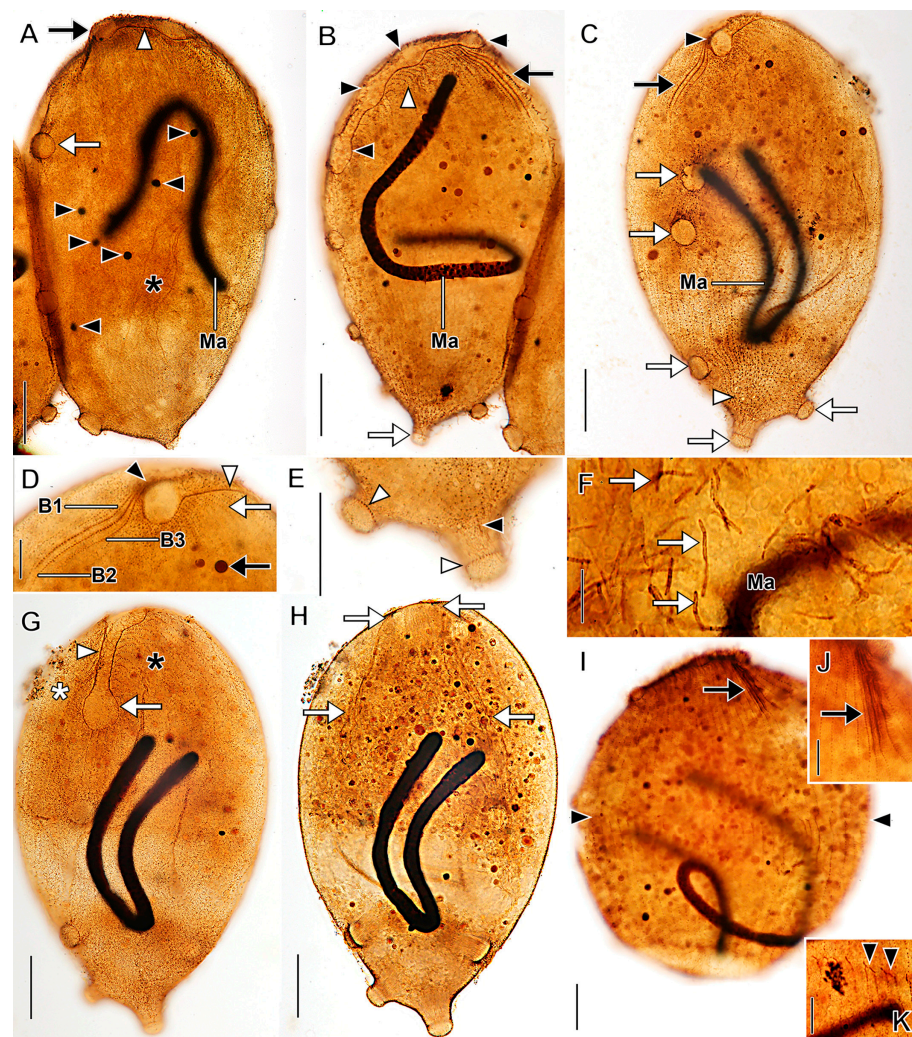


Figure 5. *Legendrea pespelicani* from VLKOV after protargol impregnation. (A) Right dorsolateral view showing the circumoral kinety (white arrowhead), an oral papilla at the dorsal end of the oral bulge (black arrow), the first dorsal tentacle (white arrow), multiple micronuclei (black arrowheads), and fibrils of the oral basket (asterisk). (B) Left ventrolateral view showing four oral papillae (black arrowheads), the anterior ends of the left somatic kineties curving ventrally (white arrowhead), dorsal brush rows extending to the left of the dorsal oral papilla (black arrow), and the posterior terminal tentacle (white arrow). (C) Right dorsolateral view showing a dorsal oral papilla (black arrowhead), the dorsal brush rows (black arrow), tentacles (white arrows), and excretory pores of the contractile vacuole (white arrowhead). (D) Detail of the same cell as (C) showing three dorsal brush rows extending to the left of the dorsal oral papilla (black arrowhead), the circumoral kinety (white arrowhead), a micronucleus (black arrow), and the right somatic kineties curving slightly dorsally (white arrow). (E) Detail of the posterior end of the cell showing the circumtentacular kinety (white arrowheads) and a somatic kinety extending onto the posterior terminal tentacle (black arrowhead). (F) Detail showing cytoplasmic endosymbionts (white arrows). (G) Left ventrolateral view showing right (white asterisk) and left (black asterisk) somatic kineties, the circumoral kinety (white arrowhead) encompassing the ventral oral papilla (white arrow). (H) Optical section showing the long, broadly conical oral basket (white arrows) extending from the oral bulge. (I) An early divider showing dorsal brush rows (black arrow) and the level of the future division furrow (black arrowheads). (J) Anterior detail, the same cell as (I), showing the dorsal brush (black arrow). (K) Detail of the same cell as (I), showing holotelokinetal morphogenesis with basal bodies proliferating from somatic kineties and curving leftward at the level of the future division furrow (black arrowheads). B1–3, dorsal brush rows 1, 2, and 3; Ma, macronucleus. Scale bars: 25 µm (A–C,G–I), 10 µm (D,F,J,K).

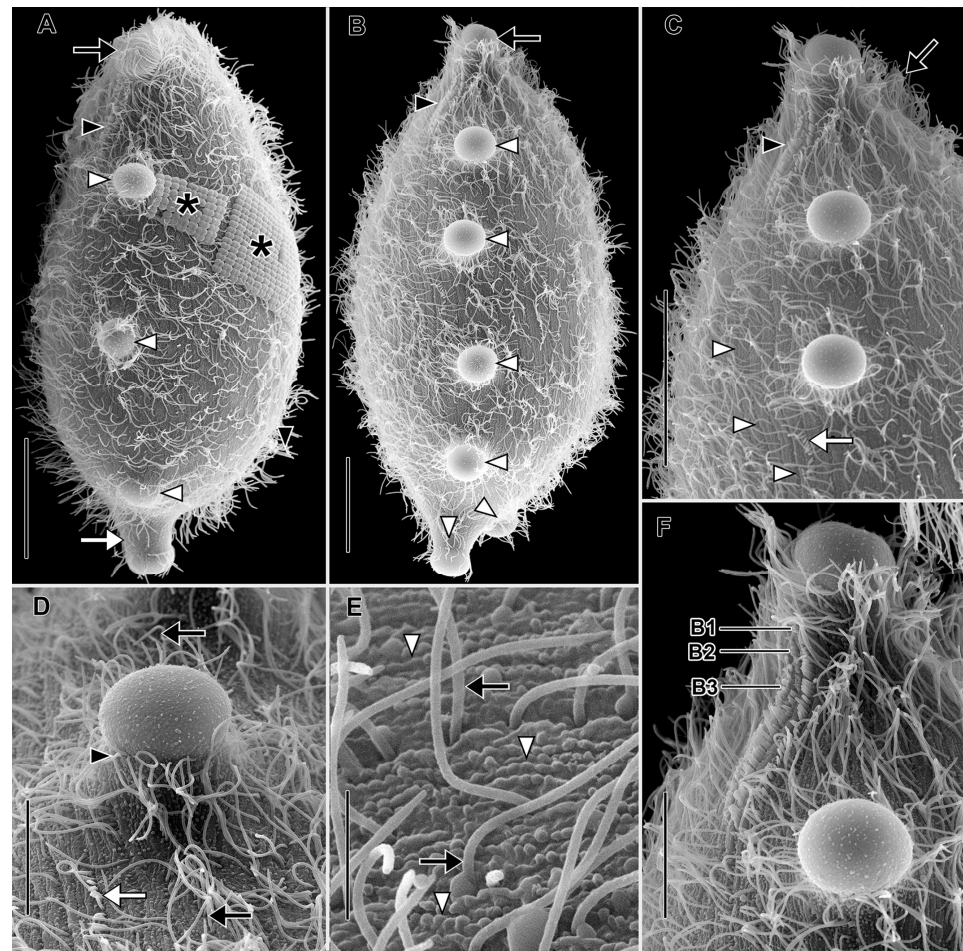


Figure 6. *Legendrea pospelicani* from VLKOV in the scanning electron microscope. (A) Dorsal view showing an oral bulge papilla (black arrow), the clavate cilia of the dorsal brush (black arrowhead), dorsal tentacles (white arrowheads), the terminal tentacle (white arrow), and *Thiopedia rosea* platelets adhering to the right side of the cell (asterisks). (B) Dorsal view showing an oral papilla (black arrow), dorsal brush rows (black arrowhead), and tentacles (white arrowheads). (C) Detail of the same cell as (B) showing the cilia of the circumoral kinety (black arrow), dorsal brush rows (black arrowhead), somatic kineties (white arrowheads), and isolated posterior groups of clavate cilia in brush row 3 (white arrow). (D) Detail showing a tentacle interrupting a somatic kinety (black arrows), an isolated group of clavate cilia posterior to dorsal brush row 3 (cf. (C)), and a ciliated circumtentacular kinety (black arrowhead). (E) Detail of the cortex showing rows of probable mucocysts (white arrowheads) and cilia of somatic monokinetids (black arrows). (F) Detail of the three inconspicuous dorsal brush rows extending to the left side of the dorsal oral papilla. B1–B3, dorsal brush rows 1–3. Scale bars: 25 μm (A–C,F), 10 μm (D), 5 μm (E).

Stomatogenesis holotelokinetal; proliferation of basal bodies first occurs in opisthe kineties in line with proter dorsal brush rows. Developing anterior ends of opisthe kineties curve ventrally (Figure 5K).

- *Legendrea ornata* (Stokes, 1887) Penard, 1914
- Original combination, *Holophrya ornata* Stokes, 1887

Amended diagnosis based on [7,10,40] and current study: With characters of genus. Size 70–180 \times 60–90 μm . Shape oblong ellipsoidal when swimming, broadly ovoidal when at rest with tentacles extended. Rows of tentacles at alternating angles on dorsal and ventral margins, commence in anterior one-fourth of cell, continuous around posterior end. Extrusome bundles about 5–7 \times 5 μm in vivo. Tentacles highly extensible, up to >25 times retracted length. Ciliary pattern distinctly enchelyodontid, unlike spathidiid pattern of

L. pespelicani, i.e., anterior ends of somatic kineties perpendicular to circumoral kinety. Ciliary rows not interrupted by tentacles as seen in *L. pespelicani*. Fewer (ten on average) circumtentacular kinety dikinetids than seen in *L. pespelicani* (35 on average). Three dorsal brush rows; B1 and B2 approximately equal in length, longer than B3.

Description based on BELG, GTUB, MOKOTP1, and SAGEGLEN (Figures 7–10; Table S3; Videos S6 and S7):

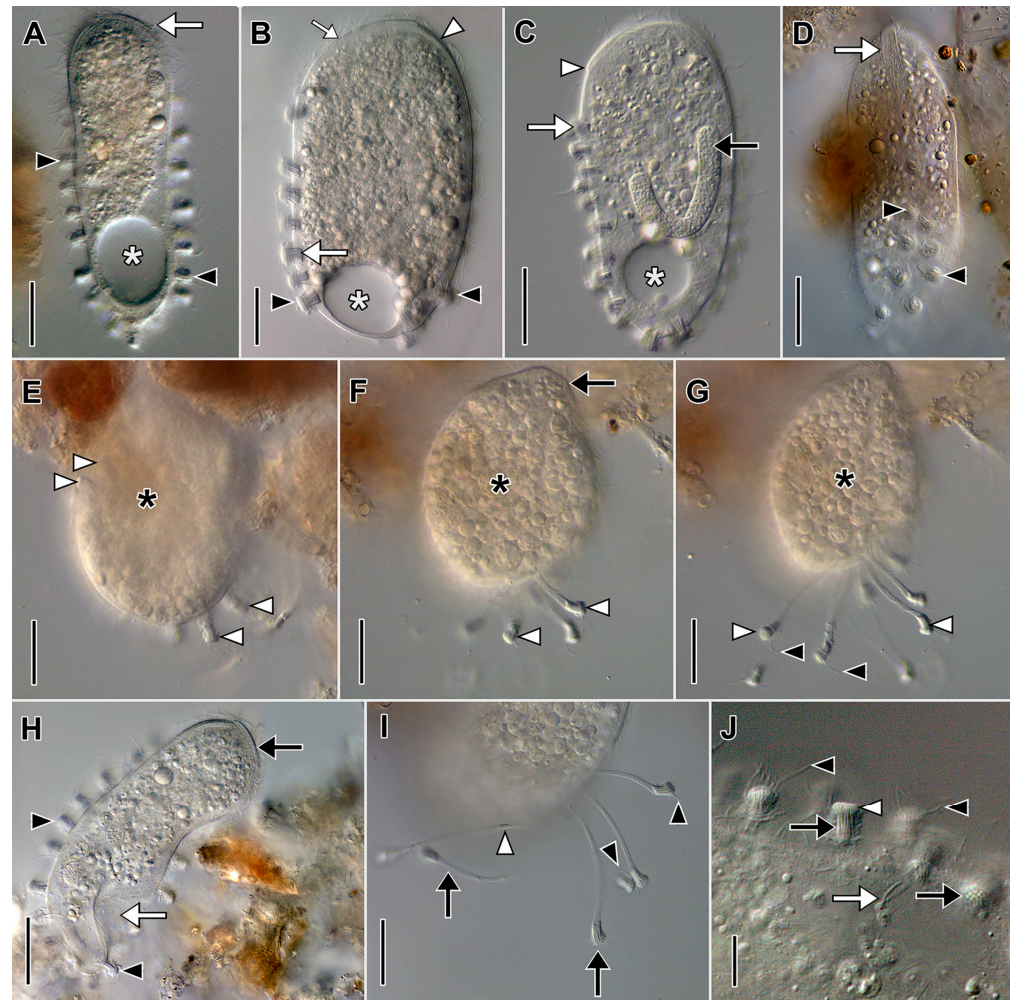


Figure 7. *Legendrea ornata* from SAGEGLEN in vivo. (A) Optical section showing the oral bulge (white arrow), retracted marginal tentacles (black arrowheads), and the contractile vacuole (asterisk). (B) Optical section showing the oral bulge (small white arrow), retracted marginal tentacles (black arrowheads), the location of the dorsal brush (white arrowhead), a tentacle extrusome bundle (white arrow), and the contractile vacuole (asterisk). (C) Optical section showing the ventral end of the oral bulge (white arrowhead), the anteriormost retracted ventral marginal tentacle (white arrow), the macronucleus (black arrow), and the contractile vacuole (asterisk). (D) Ventral view showing the oral bulge (white arrow) and retracted ventral marginal tentacles (black arrowheads). (E–G) The same cell (asterisk) during progressive extension of marginal tentacles (white arrowheads), each of which bears a ciliary wreath (black arrowheads, (G)) and a bundle of extrusomes (cf. (J)). (H) Cell showing the highly flexible cortex (white arrow), retracted marginal tentacles (black arrowheads), and the oral bulge (black arrow). (I) Detail of extended marginal tentacles (black arrows) the cilia of the circumtentacular kineties (black arrowheads), and extrusomes transiting a tentacle stalk (white arrowhead). (J) Detail of retracted marginal tentacles showing extrusomes (black arrows), ciliary wreaths of circumtentacular kineties (black arrowheads), and cytoplasmic extrusomes (white arrow). Scale bars: 25 μm (A–I), 10 μm (J).

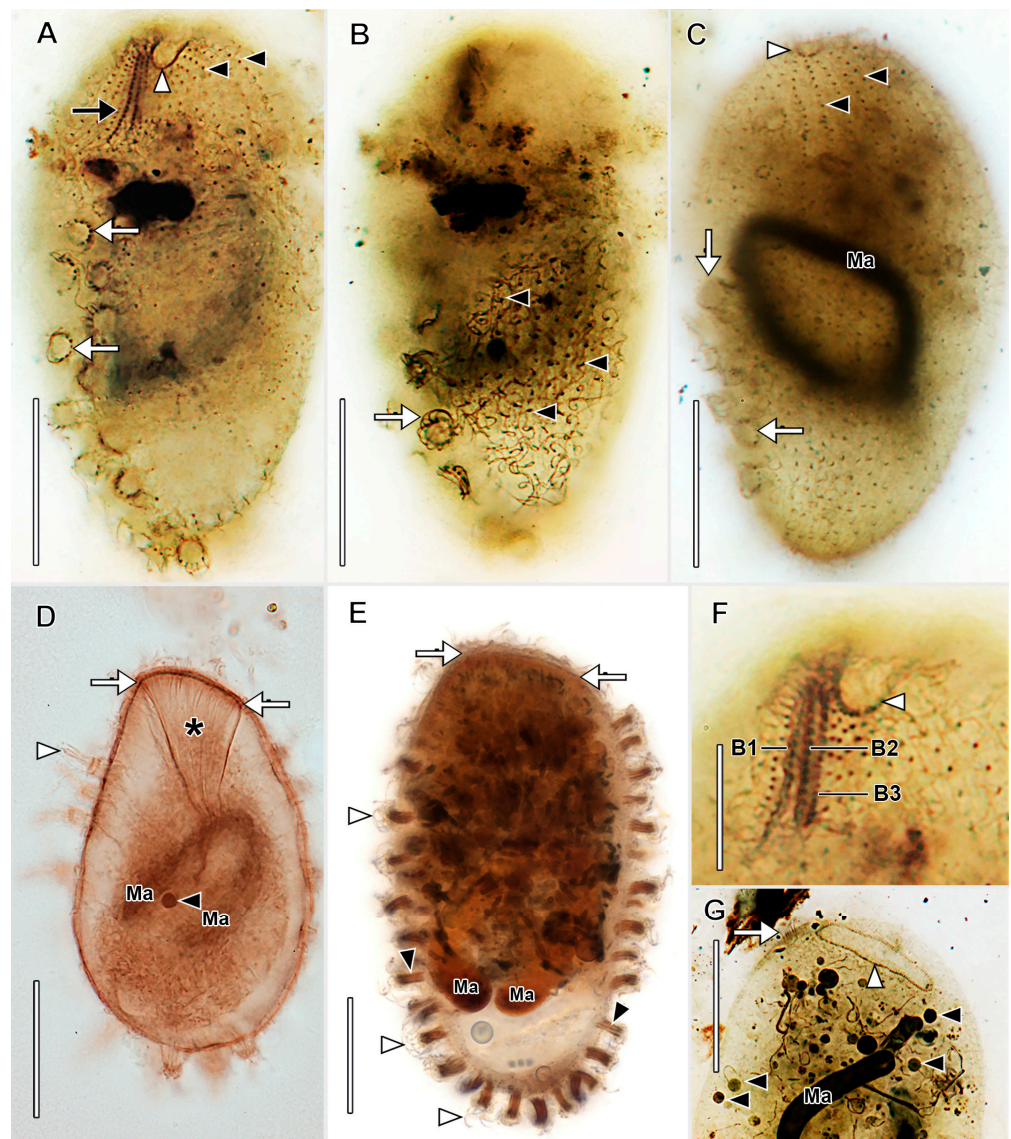


Figure 8. *Legendrea ornata* from GTUB after protargol impregnation. (A) Right dorsolateral view showing right somatic kineties (black arrowheads) perpendicularly abutting the circumoral kinety (white arrowhead), the dorsal brush (black arrow), and the dikinetids of the circumtentacular kineties (white arrows). (B) Surface view of the same cell as (A) showing circumtentacular cilia (white arrow) and longitudinal somatic kineties (black arrowheads). (C) Ventral view of the same cell as (A) showing retracted marginal tentacles (white arrows) and somatic kineties (black arrowheads) perpendicularly abutting the circumoral kinety (white arrowhead). (D) Optical section showing broad obconical oral basket (asterisk) originating from the oral bulge (between white arrows), ejected tentacular extrusomes (white arrowhead), and one of several micronuclei (black arrowhead). (E) Lateral view showing the oral bulge (between white arrows), some cilia of the marginal tentacles (white arrowheads), and tentacular extrusome bundles (black arrowheads). (F) Detail of the dorsal brush which extends to the left of the circumoral kinety (white arrowhead). (G) Dorsolateral view showing the dorsal brush (white arrow), the elliptical circumoral kinety (white arrowhead), and several micronuclei (black arrowheads). Scale bars: 25 μm (A–E,G), 10 μm (F).

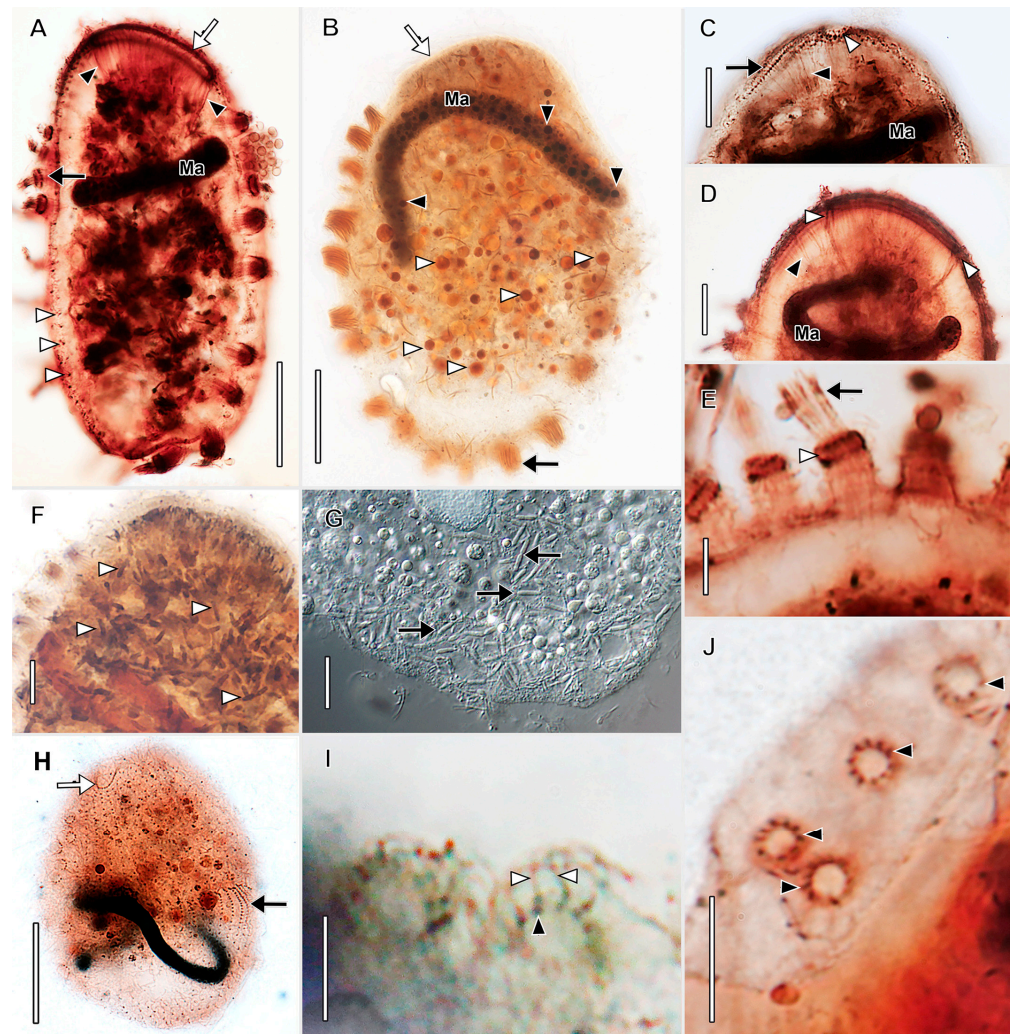


Figure 9. *Legendrea ornata* from SAGEGLEN (A,C–E,J), GTUB (H,I), and BELG (B,F) after protargol impregnation and from SAGEGLEN (G) in vivo. (A) Lateral view showing a retracted marginal tentacle with ejected extrusomes (black arrow), the obconical oral basket (between black arrowheads), the circumoral kinety (white arrow), and monokinetics of a somatic kinety (white arrowheads). (B) Optical section showing the oral bulge (white arrow), retracted marginal tentacles (black arrow), and numerous small nucleoli (black arrowheads). Numerous cytoplasmic globules (white arrowheads) make identification of micronuclei difficult. (C) Detail showing the circumoral kinety (white arrowhead). Dorsal brush row dikinetids (black arrow) give rise to oral basket nematodesmata (black arrowhead). (D) Optical section showing oral basket nematodesmata (black arrowhead) arising from dorsal brush row dikinetids to join those arising from the oral bulge (between white arrowheads). (E) Retracted marginal tentacles showing the cap (white arrowhead) and ejected extrusomes (black arrow). (F) Detail of argyrophilic cytoplasmic symbionts (white arrowheads). (G) Squashed cell showing large cytoplasmic prokaryotic endosymbionts (black arrows). (H) Dikinetids of circumtentacular kinety bear a single cilium (white arrowhead, cf. (I)). (I) Detail of a circumtentacular kinety with axially oriented dikinetids (black arrowheads) each bearing a single cilium (white arrowheads). (J) Apical view of circumtentacular cilia (black arrowheads). Ma, macronucleus. Scale bars: 25 μm (A,B), 10 μm (C,D,F,J), 5 μm (E,G–I).

With characters of genus. Size 88–141 \times 30–80 μm in vivo. Shape narrowly to broadly oblong when swimming, broadly ovoidal to almost globular when at rest with tentacles extended. Anterior end obliquely truncate; posterior end broadly rounded. Macronucleus horseshoe-shaped or tortuous strand (49–80 \times 3.5–5.5 μm), numerous nucleoli approximately 1 μm in diameter in protargol preparations, inconspicuous in vivo, multiple (2–7)

globular micronuclei (about $2.5\ \mu\text{m}$ across) in protargol preparations, not discernible in vivo (Figures 7, 8C and 9B). Contractile vacuole large, terminal, multiple excretory pores at right posterior side of cell. Two types of extrusomes: ordinary rod-shaped subcortical mucocysts (about $1 \times 0.5\ \mu\text{m}$); curved, filiform tentacular extrusomes (about $6 \times 1\ \mu\text{m}$), impregnate densely with protargol. Retracted mushroom-shaped tentacles in continuous row at alternating angles on dorsal, ventral, and posterior margin, commence in anterior one-fourth of cell, retracted tentacles with telescoping ruffled cortical collar (Figure 7A,J and Figure 10A,C); tentacles highly extensible (up to >25 times retracted length), used to immobilize prey (Video S7). Cortex flexible. Cytoplasm colorless, filled with refractive globules, prokaryotic symbionts (Figure 9F,G). Rod-shaped prokaryotic ectosymbionts in SEM preparations of some populations (Figure 10D). Swims at a moderate pace, rotating on the long axis (Video S6).

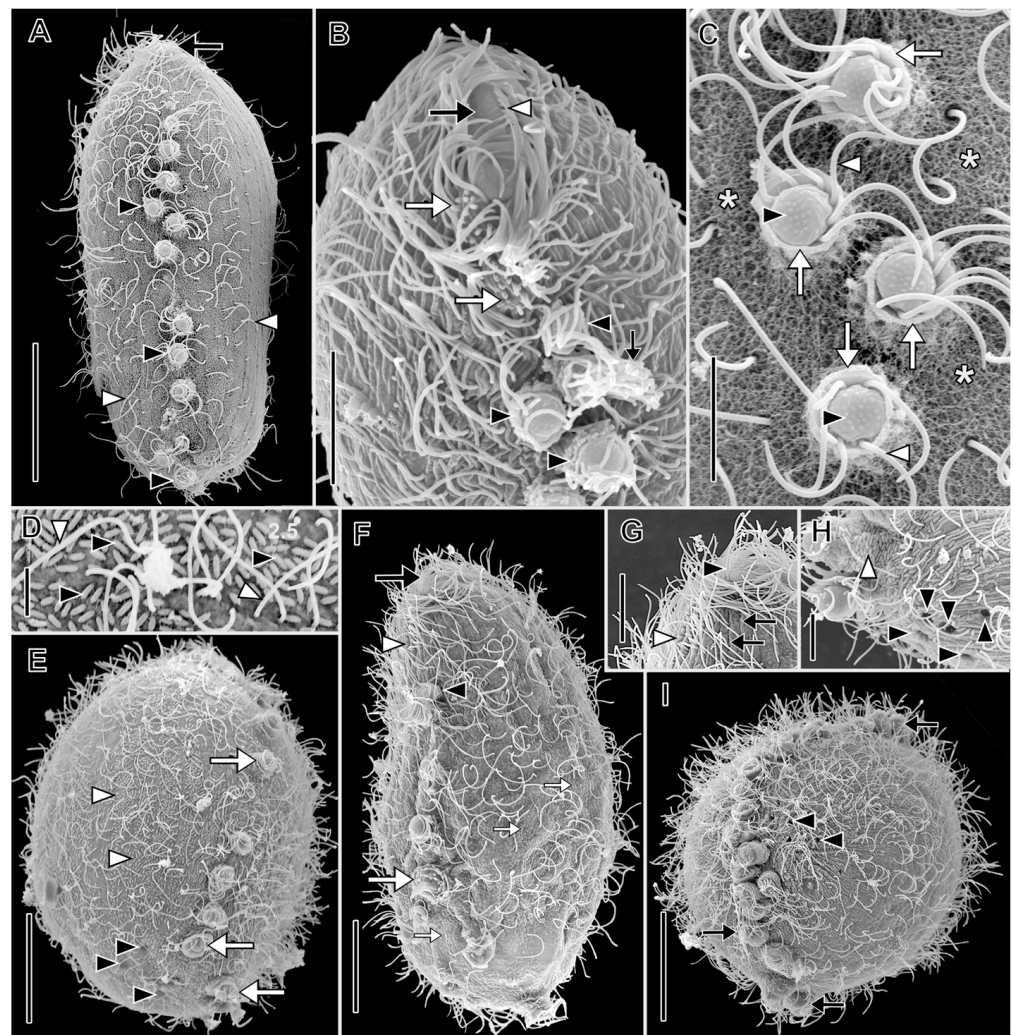


Figure 10. *Legendrea ornata* from GTUB (A,C) and BELG (B,D–I) in the scanning electron microscope. (A) Ventral view showing retracted marginal tentacles (black arrowheads), cilia of somatic monokinetics (white arrowheads), and the oral bulge (black arrow). (B) Dorsal view showing the oral bulge (black arrow), cilia of the circumoral kinety (white arrowhead), the clavate cilia of the dorsal brush (white arrows), retracted marginal tentacles (black arrowheads), and ejected tentacular extrusomes (small black arrow). (C) Detail showing docked extrusomes dotting the cap of retracted

marginal tentacles (black arrowheads), ciliary wreaths of the circumtentacular kineties (white arrowheads), the telescoped collars surrounding retracted tentacles (white arrows), and the dense reticular coating of the cortex, possibly a glycocalyx (asterisks). (D) Detail of cortical ectosymbionts (black arrowheads) and somatic cilia (white arrowheads). (E) Right ventrolateral view showing cortical symbionts (white arrowheads), retracted marginal tentacles (white arrows), and excretory pores of the contractile vacuole (black arrowheads). (F) Right dorsolateral view showing the oral bulge (black arrow), the inconspicuous dorsal brush (white arrowhead), the anteriormost dorsal marginal tentacle (black arrowhead), cortical granules—probably mucocysts (small white arrows), and the rosette-like collar of a retracted tentacle (white arrow). (G) Detail of the same cell as (F) showing the clavate cilia of the inconspicuous dorsal brush (white arrowhead), a cilium of the circumoral kinety (black arrowhead), and cortical furrows of somatic kineties (black arrows). (H) Detail of the posterior end of the cell showing cortical symbionts (white arrowhead) and the excretory pores of the contractile vacuole (black arrowheads). (I) Right posterolateral view showing retracted marginal tentacles (black arrow) and the excretory pores of the contractile vacuole (black arrowheads). Scale bars: 25 μm (A,E,F,I), 10 μm (B,G), 5 μm (C,H), 2.5 μm (D).

Somatic cilia about 12 μm long in about 30 longitudinal rows, pattern of infraciliature distinctly enchelyodontid, i.e., anterior ends of somatic kineties perpendicular to circumoral kinety. Ciliary rows not interrupted by tentacles. Dorsal brush inconspicuous; three rows of dikinetids with 3 μm long clavate cilia, brush rows commence to left of circumoral kinety; B1 and B2 of equal length (about 15 μm), B3 slightly shorter (Figure 8A,F).

Oral bulge inconspicuous, slightly oblique. Circumoral kinety narrow elliptical, composed of dikinetids. Oral bulge extrusomes not observed. Oral basket inconspicuous in vivo, obconical, extends about one-half length of cell in protargol preparations (Figures 8D and 9A,D).

Stomatogenesis holotelokinetal, basal body proliferation commences first in somatic kineties in line with dorsal brush rows (Figure 9H).

3.2. Molecular Data and Phylogenetic Analysis

Analyses of the concatenated data set revealed that the genera *Legendrea* and *Dactylochlamys* form a supported clade (bootstrap value 80, Bayesian posterior probability 1) together with *Arcuospathidium* sp. and *Apertospathula oktemae*; *Legendrea* sequences formed a fully supported clade (Figures 11 and S1).

As the 18S rRNA gene sequences of *L. loyezae* and *L. pespelicani* are identical and differ from that of *L. ornata* by only one nucleotide, the analysis based on the 18S rRNA gene did not resolve the relationships between *Legendrea* species (Figure S2), and neither did the analysis of the concatenated dataset resolve the relationships among the three *Legendrea* morphospecies. *L. ornata* MOKOTP1 and SAGEGLEN sequences cluster together. Sequences of *L. loyezae* OP352778 and *L. pespelicani* VLKOV are more closely related to each other than to *L. loyezae* MOKOTL (Figures 11 and S1). However, the published sequence of *L. loyezae* OP352778 represents only the V4 region of the 18S rRNA gene (1007 bp), while *L. pespelicani* VLKOV and *L. loyezae* MOKOTL are concatenated sequences (18S-ITS-28S). Genetic distances (uncorrected p-distances) between ITS–28S fragments (1183 bp) of *L. ornata* MOKOTP1, *L. loyezae* MOKOTL, and *L. pespelicani* VLKOV range between 0.008 and 0.009. Only amplification of the ITS–28S rRNA gene region of *Dactylochlamys* sp. MOKOTP1Q isolate was successful. Newly determined sequences are available in GenBank (accession numbers: OP985785–OP985794).

We also obtained two partial 18S rRNA gene sequences of prey gastrotrichs (family Chaetonotidae) from a cell of *L. loyezae* (MOKOTL; Figure 3B) and from the only cell of *L. ornata* from MOKOTP1 (GenBank accession numbers: OQ848030–OQ848031).

Using Sanger sequencing of 16S rRNA gene fragments, we identified two methanogenic archaeal endosymbionts as *Methanobacterium* sp. (*L. pespelicani* VLKOV) and *Methanoseta* sp. (*L. loyezae* MOKOTL) (GenBank accession numbers: OQ843028–OQ843029). Using Illumina sequencing of the V4 region of 16S rRNA gene, we identified *Methanocorpusculum*

sp. as the dominant archaeal methanogenic symbiont of *D. pisciformis* VB2A, representing around 95% of all archaeal ASVs. *Methanobacterium* sp. was the only archaeal ASV present in *L. pespelicani* VLKOV. In *L. pespelicani* VLKOV, we also identified a bacterial symbiont belonging to the Syntrophaceae (Table S4).

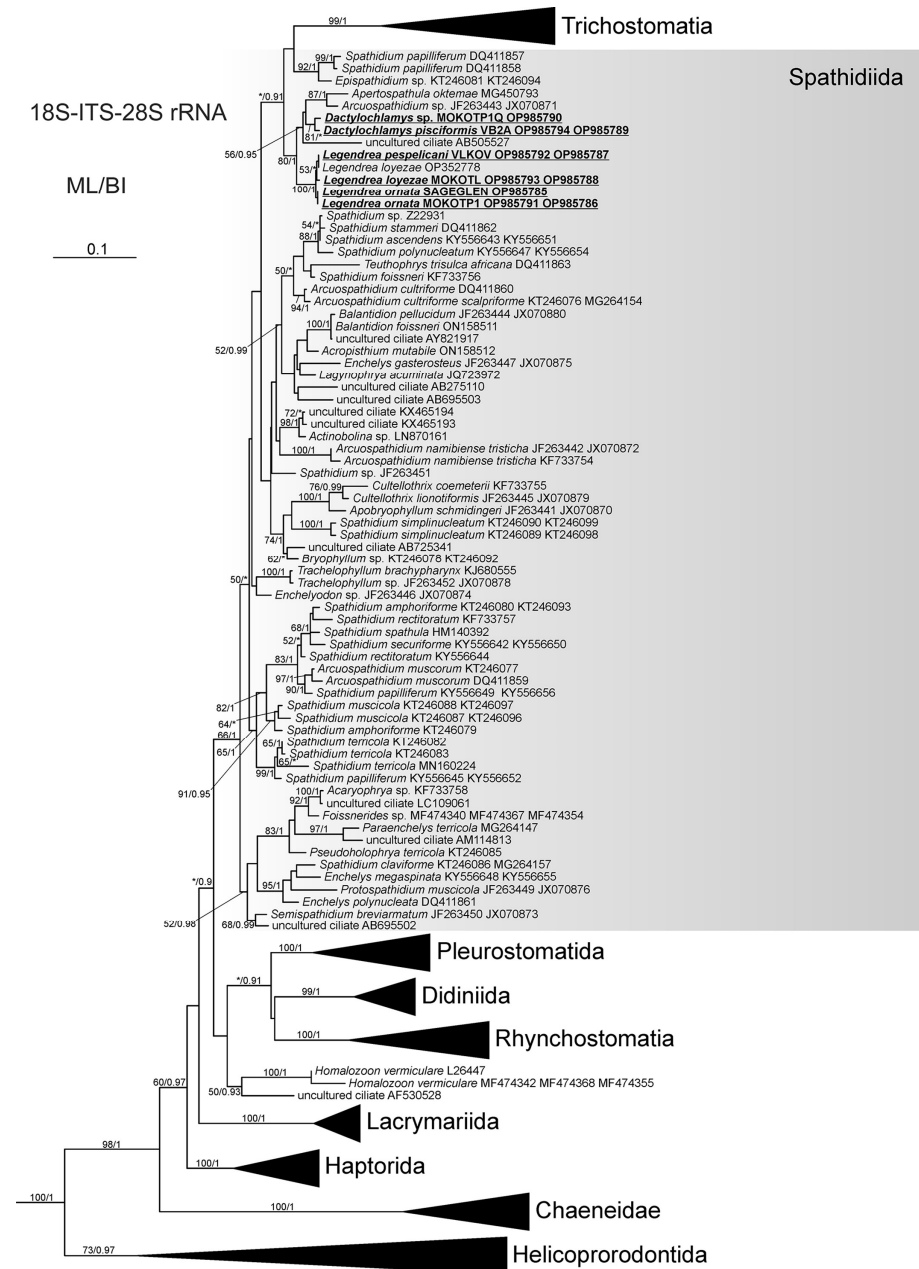


Figure 11. Maximum likelihood tree of the class Litostomatea based on 18S-ITS-28S rRNA region sequences. The tree is unrooted. The values at the branches represent statistical support in maximum likelihood bootstrap values/Bayesian posterior probabilities. Support values below 50/0.90 are not shown or depicted by an asterisk. Newly determined sequences are in bold. Accession numbers for 18S and ITS-28S GenBank sequences follow taxon names. Scale bar: 10 substitutions/100 nucleotide positions.

4. Discussion

4.1. Morphological Comparison of *Legendrea* Species and Similar Species

Legendrea pespelicani can be easily distinguished from *L. ornata* and *L. loyzeae* by size (180–210 vs. <180 μm), cell shape (broadly spatulate vs. oblong, resp. broadly obovate), and by possession of oral papillae (present vs. absent). *L. pespelicani* also differs from

L. ornata by number of tentacles (4–8 vs. 10–43), number of circumoral kineties (30 vs. 10 in average), number of somatic kineties (66–70 vs. 28–36), and the disposition of the ciliary rows (interrupted by tentacles vs. deviating around the tentacles). *L. loyzae* can be distinguished from *L. ornata* by the position of tentacles (bundle at the posterior vs. margin of the cell on $\frac{3}{4}$ of the cell length), and from both other species by the eccentric posterior contractile vacuole which appears as two vacuoles due to median cleft at posterior. All *Legendrea* species are different to any other spathidiid in terms of tentacles (present vs. absent), except *Dactylochlamys pisciformis*, which are not similar to those of *Legendrea* (very slender, not ciliated vs. thick with circumtentacular kineties). *L. pespelicani* differs from *Spathidium papilliferum* in morphology of the oral papillae (circumtentacular kineties present vs. absent).

4.2. Remarks on the Rarity and Ecology of *Dactylochlamys* and *Legendrea*

Both *Dactylochlamys* and *Legendrea* spp. have been very rarely reported, although Lauterborn and Penard suggested that the populations could be quite abundant [9,37]. Our experience was similar: the VB2A sample was unusually rich in *Dactylochlamys* (approx. 4 cells/mL of water and sediment), but the abundance quickly declined in several days, and we were unable to maintain the ciliate in long-term culture. In other cases (MRATIN, MOKOTP1Q), only a few cells were found in the whole volume of a 50 mL sample. In the case of *Dactylochlamys*, Penard cautioned about possible misidentification, because some swimmers of suctorian ciliates (Phyllopharyngea: Suctoria) (e.g., *Enchelyomorpha vermicularis* Smith, 1899) appear similar in vivo (compare Figure 1F,I) [9]. Thus, mentions in the literature not accompanied by illustrations are questionable, e.g., [41,42]. In the case of *Legendrea*, we found two relatively rich localities in the Czech Republic and one in the USA; other known localities are, for example, in France, Germany, Belgium, and Poland. This might suggest that the rarity of *Dactylochlamys* and *Legendrea* is rather a matter of specific habitat conditions than endemism.

Interestingly, gastrotrich rRNA gene partial sequences (family Chaetonotidae) were recovered from cells of *L. loyzae* and *L. ornata*, indicating ingestion of gastrotrichs as prey. The process of *L. ornata* from sediments of a German freshwater pond catching and digesting a gastrotrich (family Chaetonotidae) is the first documentation of the role played by the tentacles in prey capture (Video S7). Chaetonotidae is a species-rich and widely distributed gastrotrich family that commonly inhabits hypoxic lacustrine sediments [43]. Although chaetonotid gastrotrich 18S rRNA gene sequences were the only eukaryotic contaminants from *Legendrea*, the importance of gastrotrichs in the diet of *Legendrea* species remains unknown.

4.3. Phylogenetic Analysis and the Relationship of Tentaculiferous Ciliates

A recent report (8) included a 994 bp V4–V9 rRNA region sequence from *L. loyzae*. Phylogenetic analysis could not resolve a position of *Legendrea* within Haptorida. The problems with attempting to resolve relationships within Litostomatea based on analysis of the rRNA cistron have been emphasized previously [44,45]. Consistent with the studies mentioned above, we did not succeed in resolving the internal relationships among *Legendrea* species in spite of addition of two more markers, i.e., using three times more positions in comparison to [8].

Despite pronounced morphological differences, all three identified *Legendrea* species have identical (*L. loyzae* and *L. pespelicani*) or almost identical (*L. ornata*) 18S rRNA gene sequences. However, the existence of the three *Legendrea* morphospecies is further supported by the analysis based on additional molecular markers; namely, part of the ITS region and part of the 28S rRNA gene. Clustering of *L. loyzae* OP352778 with *L. pespelicani* was interpreted as an artifact due to the short length of the former (1007 nucleotides) and ambiguous sites in both of the sequences of *L. loyzae*. This view is also supported by the p-distances of the ITS–28S fragments of each of the three *Legendrea* species, which range from 0.008 to 0.009. On the other hand, Jankowski even erected a monotypic genus for each

of the three *Legendrea* species solely on morphology, but we consider with respect to the morphological and molecular analysis presented above [46].

We also obtained a partial ITS-28S rRNA gene sequence of a second *Dactylochlamys* population (MOKOTP1Q), but the material was insufficient for morphometric analysis. Molecular data and in vivo observation suggest that it is possibly a new species (Video S9).

Our analysis showed that *Dactylochlamys* and *Legendrea* are not closely related to *Actinobolina*, contradicting the traditional notion of the family Actinobolinidae, comprising the genera *Actinobolina*, *Belonophrya*, *Legendrea*, and *Dactylochlamys*, based on the presence of tentacle-like structures which have evolved independently [1,10,47]. As noted previously, homoplasies are rife throughout the Spathidiidae and, together with many pleiomorphies, have so far obscured the evolutionary relationships in the group [44,48–50]. Interestingly, *Dactylochlamys* and *Legendrea* are members of the same well-supported clade despite their obvious morphological differences. The other members of the clade (i.e., *Apertospathula oktemae* and an undescribed *Arcuospathidium* sp.) belong to spathidiid genera which do not bear any tentacle-like structures [2]. *Spathidium papilliferum* Kahl, 1930, another only distantly related spathidiid, has oral bulge papillae superficially similar to those of *L. pespelicani* but lacking circumtentacular kineties [10,48]. Analysis also showed that a supported clade including *S. papilliferum* (DQ411857, DQ411858; morphologically uncharacterized population) and an *Epispathidium* species (KT246081, KT246094; undescribed) are not closely related to the other *S. papilliferum* (KY556645, KY556652), suggesting possible misidentification (Figure 11). Thus, the diversity of tentacle- or papillae-bearing spathidiids could be even higher than currently indicated. The genus *Belonophrya* is highly similar to *Actinobolina*, but molecular data and ultrastructural details of its tentacles are still unavailable [51]. Another tentacle-bearing ciliate, *Holophrya ornata* is now synonymized with *Legendrea bellerophon* based on its morphological characteristics (Figure 12) [40].

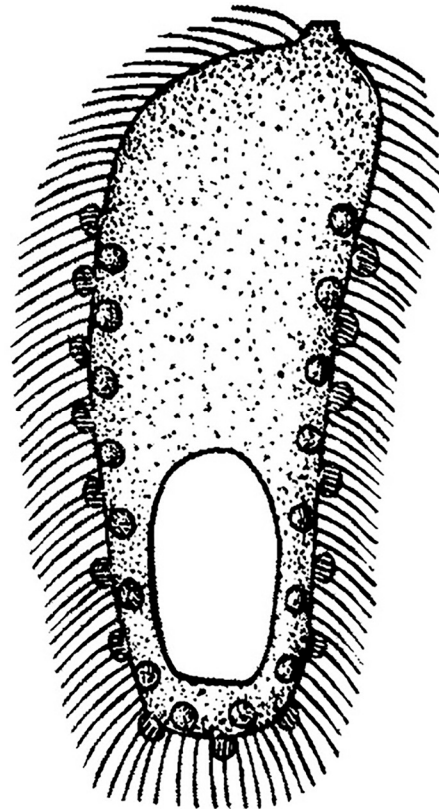


Figure 12. Illustration of *Holophrya ornata* from Stokes (1887). Cell length 100 μm .

Given the complex relationships between tentaculiferous lineages in Spathidiidae or Haptoria, it is not surprising that tentacles of other litostomateans are also likely not

homologous. Tentacles in the family Mesodiniidae, possibly a sister group to Litostomatea, are placed anteriorly, are reinforced by a cylindrical structure of 14 microtubules, and bear extrusomes [1,52,53]. Another tentacle-bearing species with unclear phylogenetic position is *Enchelyomorpha vermicularis*, once included in Actinobolnidae, tentacles of which are also reinforced by microtubules and do not bear extrusomes, which is now considered to be the swarmer of a globular suctorian on morphological grounds but has not yet been sequenced [1,54]. Tentacles of the members of the class Phyllopharyngea have a completely different morphology compared to both *Legendrea* and *Dactylochlamys*. Typical suctorian feeding tentacles are formed by two concentric cylinders of microtubules, the inner one being reinforced by microtubule fibrils, and the outer with various taxon-specific microtubular structures [1,55]. Although, as indicated by their name, suctorians have been assumed to “suck” cell contents from their prey, this mechanism has been cast into doubt by Rudzinska [56]. In the parasitic subclass Rhynchodia, only a single sucking tentacle-like structure, probably a transformed cytostome, is present [1].

4.4. Putative Prokaryotic Endosymbionts

Using Sanger sequencing of the partial 16S rRNA gene, we identified putative methanogenic endosymbionts of *L. pospelicani* as *Methanobacterium* sp. and *Methanosaeta* sp. in *L. loyzae*. Using Illumina sequencing, we corroborated the identity of the archaeal symbiont of *L. pospelicani* as *Methanobacterium* sp. and identified the archaeal symbiont of *Dactylochlamys pisciformis* as *Methanocorpusculum* sp. Autofluorescence typical of archaeal methanogens was also observed in *Dactylochlamys* (Video S8) [57]. Interestingly, it seems that there is some symbiont diversity among the studied species, where genera belonging to the same clade and even each of the *Legendrea* species harbor different methanogenic symbionts. Methanogenic Archaea commonly form syntrophic symbioses with anaerobic ciliates using the hydrogen and acetate produced by the host mitochondria for their metabolism, e.g., [21,58–60]. This suggests that both *Dactylochlamys* and *Legendrea* are most likely facultative or obligate anaerobes, potentially having hydrogen-producing mitochondria. The role of these prokaryotes as endosymbionts requires confirmation by fluorescence in situ hybridization and/or transmission electron microscopy. Nevertheless, our results indicate that both *Dactylochlamys* and *Legendrea* represent a novel anaerobic lineage of ciliates. Interestingly, in addition to archaeal symbionts, we also identified a putative bacterial symbiont related to the family Syntrophaceae. The Syntrophaceae are strictly anaerobic and grow only in the presence of hydrogen-utilizing partners, such as archaeal methanogens [61]. Further investigations of symbiotic interactions between the host, archaeal, and bacterial endosymbionts in *Legendrea* are needed.

4.5. The Role of Citizen Science in Ciliatology

Taxonomic and biogeographic studies of a wide variety of groups, including protists, have always been plagued by the problem of undersampling. This fact, in part, underlies the uncertainty and contentiousness associated with such topics as protist endemism [62–64]. Since the number of academic professionals dedicated to and funded for mainly taxonomic work has rapidly declined, the importance of the much larger population of “expert amateurs” (interested individuals without formal academic credentials in the particular specialty) in species identification, specimen collection, ecology, and biogeographical data collection has come into clearer focus [65–70]. The role of the expert amateur was central to science world-wide prior to the professionalization of science in the early 20th century, after which contributions by non-academics were increasingly ignored or criticized as inferior. Alfred Kahl, one of the most notable ciliatologists of the last century, a high school teacher by training, was probably an unfortunate object of this developing attitude [38,71]. Although a formal definition of “citizen-science” infers that it occurs mainly as an activity in collaboration with, or under the direction of, academic professionals usually as part of structured projects [72], we consider the data generated by expert amateurs working independently to be of considerable value, especially with regard to rare taxa such as

Legendrea. Most of the information that has accrued in the century since the first description of the genus *Legendrea* has been gathered almost exclusively by expert amateurs and made publicly available in online forums and social media. The study of Weiss et al. and this study are perfect examples of the fruitfulness of such cooperation [8].

5. Conclusions

Although both genera, *Legendrea* and *Dactylochlamys*, presented in this study are considered to be remarkably rare, we were able to collect enough data to not only corroborate their phylogenetic position close to or within Spathidiidae but also revealed that both genera are closely related to each other despite apparent differences in their tentacle-like structures. We studied their morphology with modern methods and found out that these two ciliate genera are in fact anaerobes harboring prokaryotic endosymbionts. Our work demonstrates that for studying rare organisms, both modern single-cell methods and the contribution of citizen science are essential. Thus, we encourage the increasing collaboration of academic professionals with their expert amateur counterparts, inclusion of their data in peer-reviewed research publications, and acknowledgement of their contributions.

Supplementary Materials: The following supporting information can be downloaded at: <https://www.mdpi.com/article/10.3390/biology12050707/s1>, Figure S1: Maximum likelihood tree of the class Litostomatea based on 18S-ITS-28S rRNA region sequences, Figure S2: Maximum likelihood tree of the class Litostomatea based on 18S rRNA gene sequences; Table S1: Morphometric table of *Dactylochlamys pisciformis*, Table S2: Morphometric table of *Legendrea pespelicani*, Table S3: Morphometric table of *Legendrea ornata*, Table S4: Illumina consensus nucleotide sequences of putative prokaryotic symbionts; List of Videos S1–S9.

Author Contributions: Conceptualization, O.P. and W.A.B.; methodology, O.P., W.A.B., D.M.-S., K.P. and I.Č.; software, O.P., W.A.B., D.M.-S., K.P. and I.Č.; investigation, O.P., W.A.B., D.M.-S., K.P., M.M., M.-M.S. and I.Č.; writing—original draft preparation, O.P. and W.A.B.; writing—review and editing, O.P., W.A.B., D.M.-S., K.P. and I.Č.; visualization, O.P., W.A.B., D.M.-S., K.P. and I.Č.; supervision, I.Č. All authors have read and agreed to the published version of the manuscript.

Funding: This research was funded by The Czech Science Foundation (GACR), grant number 23-06004S and GAUK grant number 365021. Daniel Méndez-Sánchez and Kateřina Poláková acknowledge support from the project “Grant Schemes at CU” (reg. no. CZ.02.2.69/0.0/0.0/19_073/0016935).

Institutional Review Board Statement: Not applicable.

Informed Consent Statement: Not applicable.

Data Availability Statement: The data presented in this study are openly available in the Supplementary Material or GenBank at <https://www.ncbi.nlm.nih.gov/genbank/>, accessed on 15 March 2023, reference number OP985785–OP985794 and OQ843028–OQ848031.

Conflicts of Interest: The authors declare no conflict of interest.

References

- Lynn, D.H. *The Ciliated Protozoa: Characterization, Classification, and Guide to the Literature*; Springer: Dordrecht, Germany, 2008.
- Foissner, W.; Xu, K. Monograph of the Spathidiida (Ciliophora, Haptoria). *Monogr. Biol.* **2007**, *81*, 1–485.
- Cedrola, F.; Senra, M.V.X.; Rossi, M.F.; Fregulia, P.; D’Agosto, M.; Dias, R.J.P. Trichostomatid ciliates (Alveolata, Ciliophora, Trichostomatia) systematics and diversity: Past, present and future. *Front. Microbiol.* **2020**, *10*, 2967. [[CrossRef](#)]
- Foissner, W.; Berger, H.; Schaumburg, H. *Identification and Ecology of Limnetic Plankton Ciliates*; Informationsberichte des Bayerischen Landesamtes für Wasserwirtschaft: Deggendorf, Germany, 1999.
- Kreutz, M.; Foissner, W. The *Sphagnum* ponds of Simmelried in Germany: A biodiversity hot-spot for microscopic organisms. *Protozool. Monogr.* **2006**, *3*, 1–267.
- Jiang, L.; Wang, C.; Zhuang, W.; Li, S.; Hu, X. Taxonomy, phylogeny, and geographical distribution of the little-known *Helicoprordon multinucleatum* Dragesco, 1960 (Ciliophora, Haptorida) and key to species within the genus. *Eur. J. Protistol.* **2021**, *78*, 125769. [[CrossRef](#)] [[PubMed](#)]
- Penard, E. Un curieux infusoire *Legendrea bellerophon*. *Rev. Suisse Zool.* **1914**, *22*, 407–432.
- Weiss, J.; Andreou, D.; Esteban, G.F. The Extraordinarily rare ciliate *Legendrea loyzeae* Fauré-Fremiet, 1908 (Haptoria, Ciliophora). *Protist* **2022**, *173*, 125912. [[CrossRef](#)] [[PubMed](#)]

9. Penard, E. *Études sur les Infusoires d'Eau Douce*; George & Cie: Geneva, Switzerland, 1922.
10. Kahl, A. Urtiere oder Protozoa I: Wimpertiere oder Ciliata (Infusoria) I. Allgemeiner Teil und Prostomata. *Die Tierwelt Dtschl. Und Der Angrenz. Meerest. Nach Ihren Merkmalen Und Nach Ihrer Lebensw.* **1930**, *18*, 1–186.
11. Foissner, W.; Xu, K.; Kreutz, M. The Apertospathulidae, a new family of haptorid ciliates (Protozoa, Ciliophora). *J. Eukaryot. Microbiol.* **2005**, *52*, 360–373. [[CrossRef](#)] [[PubMed](#)]
12. Bourland, W.A.; Wendell, L.; Hampikian, G. Morphologic and molecular description of *Metopus fuscus* Kahl from North America and new rDNA sequences from seven metopids (Armophorea, Metopidae). *Eur. J. Protistol.* **2014**, *50*, 213–230. [[CrossRef](#)]
13. Dieckmann, J. An improved protargol impregnation for ciliates yielding reproducible results. *Eur. J. Protistol.* **1995**, *31*, 372–382. [[CrossRef](#)]
14. Foissner, W. An update of 'basic light and scanning electron microscopic methods for taxonomic studies of ciliated protozoa'. *Int. J. Syst. Evol. Microbiol.* **2014**, *64*, 271–292. [[CrossRef](#)] [[PubMed](#)]
15. Pan, X.; Bourland, W.A.; Song, W. Protargol synthesis: An in-house protocol. *J. Eukaryot. Microbiol.* **2013**, *60*, 609–614. [[CrossRef](#)] [[PubMed](#)]
16. Strüder-Kypke, M.C.; Lynn, D.H. Sequence analyses of the small subunit rRNA gene confirm the paraphyly of oligotrich ciliates sensu lato and support the monophyly of the subclasses Oligotrichia and Choreotrichia (Ciliophora, Spirotrichea). *J. Zool.* **2003**, *260*, 87–97. [[CrossRef](#)]
17. Medlin, L.; Elwood, H.J.; Stickel, S.; Sogin, M.L. The characterization of enzymatically amplified eukaryotic 16S-like rRNA-coding regions. *Gene* **1988**, *7*, 491–499. [[CrossRef](#)] [[PubMed](#)]
18. Jerome, C.A.; Lynn, D.H.; Simon, E.M. Description of *Tetrahymena empidokyrea* n. sp., a new species in the *Tetrahymena pyriformis* sibling species complex (Ciliophora, Oligohymenophorea), and an assessment of its phylogenetic position using small-subunit rRNA sequences. *Can. J. Zool.* **1996**, *74*, 1898–1906. [[CrossRef](#)]
19. Miao, M.; Warren, A.; Song, W.; Wang, S.; Shang, H.; Chen, Z. Analysis of the internal transcribed spacer 2 (ITS2) region of scuticociliates and related taxa (Ciliophora, Oligohymenophorea) to infer their evolution and phylogeny. *Protist* **2008**, *159*, 519–533. [[CrossRef](#)]
20. Pawlowski, J. Introduction to the molecular systematics of foraminifera. *Micropaleontology* **2000**, *46*, 1–12. Available online: <http://www.jstor.org/stable/1486176> (accessed on 22 December 2022).
21. van Hoek, A.H.; van Alen, T.A.; Sprakel, V.S.; Leunissen, J.A.; Brigge, T.; Vogels, G.D.; Hackstein, J.H. Multiple acquisition of methanogenic archaeal symbionts by anaerobic ciliates. *Mol. Biol. Evol.* **2000**, *17*, 251–258. [[CrossRef](#)]
22. Irbis, C.; Ushida, K. Detection of methanogens and proteobacteria from a single cell of rumen ciliate protozoa. *J. Gen. Appl. Microbiol.* **2004**, *50*, 203–212. [[CrossRef](#)]
23. Apprill, A.; McNally, S.; Parsons, R.; Weber, L. Minor revision to V4 region SSU rRNA 806R gene primer greatly increases detection of SAR11 bacterioplankton. *Aquat. Microb. Ecol.* **2015**, *75*, 129–137. [[CrossRef](#)]
24. Parada, A.E.; Needham, D.M.; Fuhrman, J.A. Every base matters: Assessing small subunit rRNA primers for marine microbiomes with mock communities, time series and global field samples. *Environ. Microbiol.* **2016**, *18*, 1403–1414. [[CrossRef](#)] [[PubMed](#)]
25. Callahan, B.J.; McMurdie, P.J.; Rosen, M.J.; Han, A.W.; Johnson, A.J.; Holmes, S.P. DADA2: High-resolution sample inference from Illumina amplicon data. *Nat. Methods* **2016**, *13*, 581–583. [[CrossRef](#)]
26. Bolyen, E.; Rideout, J.R.; Dillon, M.R.; Bokulich, N.A.; Abnet, C.C.; Al-Ghalith, G.A.; Alexander, H.; Alm, E.J.; Arumugam, M.; Asnicar, F.; et al. Reproducible, interactive, scalable and extensible microbiome data science using QIIME 2. *Nat. Biotechnol.* **2019**, *37*, 852–857. [[CrossRef](#)] [[PubMed](#)]
27. Bokulich, N.A.; Kaehler, B.D.; Rideout, J.R.; Dillon, M.; Bolyen, E.; Knight, R.; Huttley, G.A.; Gregory Caporaso, J. Optimizing taxonomic classification of marker-gene amplicon sequences with QIIME 2's q2-feature-classifier plugin. *Microbiome* **2018**, *6*, 90. [[CrossRef](#)] [[PubMed](#)]
28. Quast, C.; Pruesse, E.; Yilmaz, P.; Gerken, J.; Schweer, T.; Yarza, P.; Peplies, J.; Glöckner, F.O. The SILVA ribosomal RNA gene database project: Improved data processing and web-based tools. *Nucleic Acids Res.* **2013**, *41*, D590–D596. [[CrossRef](#)] [[PubMed](#)]
29. Gentekaki, E.; Kolisko, M.; Boscaro, V.; Bright, K.J.; Dini, F.; Di Giuseppe, G.; Gong, Y.; Miceli, C.; Modeo, L.; Molestina, R.E.; et al. Large-scale phylogenomic analysis reveals the phylogenetic position of the problematic taxon *Protocruzia* and unravels the deep phylogenetic affinities of the ciliate lineages. *Mol. Phylogenet. Evol.* **2014**, *78*, 36–42. [[CrossRef](#)]
30. Katoh, K.; Misawa, K.; Kuma, K.; Miyata, T. MAFFT: A novel method for rapid multiple sequence alignment based on fast Fourier transform. *Nucleic Acids Res.* **2002**, *30*, 3059–3066. [[CrossRef](#)]
31. Larsson, A. AliView: A fast and lightweight alignment viewer and editor for large datasets. *Bioinformatics* **2014**, *30*, 3276–3278. [[CrossRef](#)]
32. Darriba, D.; Posada, D.; Kozlov, A.M.; Stamatakis, A.; Morel, B.; Flouri, T. ModelTest-NG: A new and scalable tool for the selection of DNA and protein evolutionary models. *Mol. Biol. Evol.* **2020**, *37*, 291–294. [[CrossRef](#)]
33. Flouri, T.; Izquierdo-Carrasco, F.; Darriba, D.; Aberer, A.J.; Nguyen, L.T.; Minh, B.Q.; Von Haeseler, A.; Stamatakis, A. The phylogenetic likelihood library. *Syst. Biol.* **2015**, *64*, 356–362. [[CrossRef](#)]
34. Kozlov, A.M.; Darriba, D.; Flouri, T.; Morel, B.; Stamatakis, A. RAXML-NG: A fast, scalable and user-friendly tool for maximum likelihood phylogenetic inference. *Bioinformatics* **2019**, *35*, 4453–4455. [[CrossRef](#)]

35. Ronquist, F.; Teslenko, M.; Van Der Mark, P.; Ayres, D.L.; Darling, A.; Höhna, S.; Larget, B.; Liu, L.; Suchard, M.A. MrBayes 3.2: Efficient Bayesian phylogenetic inference and model choice across a large model space. *Syst. Biol.* **2012**, *61*, 539–542. [[CrossRef](#)] [[PubMed](#)]
36. Warren, D.L.; Geneva, A.J.; Lanfear, R. RWTY (R We There Yet): An R package for examining convergence of Bayesian phylogenetic analyses. *Mol. Biol. Evol.* **2017**, *34*, 1016–1020. [[CrossRef](#)] [[PubMed](#)]
37. Lauterborn, R. Die “sapropelische” Lebewelt. *Zool. Anz.* **1901**, *24*, 50–55.
38. Wetzel, A. Der Faulschlamm und seine ziliaten Leitformen. *Z. Morphol. Ökol. Tiere* **1928**, *13*, 179–328. [[CrossRef](#)]
39. Fauré-Fremiet, E. Sur deux Infusoires nouveaux de la famille des Trachelidae. *Bull. Soc. Zool. Fr.* **1908**, *33*, 13–16.
40. Stokes, A.C. Notices of new fresh-water infusoria. *Proc. Am. Philos. Soc.* **1887**, *24*, 244–255.
41. Babko, R.V.; Kuzmina, T.M. Spatial distribution of ciliates (Protista, Ciliophora) in the river Bityza (Dnieper basin). *Vestnik Zoologii* **1999**, *33*, 83–89.
42. Lackey, J.B. The Plankton Algae and Protozoa of Two Tennessee Rivers. *Am. Midl. Nat.* **1942**, *27*, 191–202. [[CrossRef](#)]
43. Strayer, D. The benthic micrometazoans of Mirror Lake, New Hampshire. *Arch. Hydrobiol.* **1985**, *72*, 287–426.
44. Vd’áčný, P.; Bourland, W.A.; Orsi, W.; Epstein, S.S.; Foissner, W. Genealogical analyses of multiple loci of litostomatean ciliates (Protista, Ciliophora, Litostomatea). *Mol. Phylogenet. Evol.* **2012**, *65*, 397–411. [[CrossRef](#)] [[PubMed](#)]
45. Vd’áčný, P.; Breiner, H.W.; Yashchenko, V.; Dunthorn, M.; Stoeck, T.; Foissner, W. The chaos prevails: Molecular phylogeny of the Haptoria (Ciliophora, Litostomatea). *Protist* **2014**, *165*, 93–111. [[CrossRef](#)] [[PubMed](#)]
46. Jankowski, A.W. Phylum Ciliophora Doflein, 1901. In *Protista. Part 2, Handbook on Zoology*; Alimov, A.F., Ed.; Russian Academy of Sciences, Zoological Institut: St. Petersburg, Russia, 2007; pp. 371–993.
47. Corliss, J.O. *The Ciliated Protozoa. Characterization, Classification and Guide to the Literature*; Pergamon Press: New York, NY, USA, 1979.
48. Jang, S.W.; Vd’áčný, P.; Shazib, S.U.A.; Shin, M.K. Linking morphology and molecules: Integrative taxonomy of spathidiids (Protista: Ciliophora: Litostomatea) from Korea. *J. Nat. Hist.* **2017**, *51*, 1–36. [[CrossRef](#)]
49. Rajter, L.; Vd’áčný, P. Rapid radiation, gradual extinction and parallel evolution challenge generic classification of spathidiid ciliates (Protista, Ciliophora). *Zool. Scr.* **2015**, *45*, 200–223. [[CrossRef](#)]
50. Ylidiz, I. Morphology and phylogeny of *Apertospathula oktemae* n. sp. (Ciliophora, Haptoria, Spathidiida) from Lake Van, Turkey. *Eur. J. Protistol.* **2018**, *66*, 1–8. [[CrossRef](#)]
51. Holt, P.; Corliss, J.O. Pattern variability in microtubular arrays associated with the tentacles of *Actinobolina* (Ciliata: Gymnostom- atida). *J. Cell Biol.* **1973**, *58*, 213–219. [[CrossRef](#)]
52. Lasek-Nesselquist, E.; Johnson, M.D. A phylogenomic approach to clarifying the relationship of *Mesodinium* within the Ciliophora: A case study in the complexity of mixed-species transcriptome analyses. *Genome Biol. Evol.* **2019**, *11*, 3218–3232. [[CrossRef](#)]
53. Lindholm, T.; Lindroosand, P.; Mörk, A.C. Ultrastructure of the photosynthetic ciliate *Mesodinium rubrum*. *Biosystems* **1988**, *21*, 141–149. [[CrossRef](#)]
54. Foissner, W.; Foissner, I. Fine structure and systematic position of *Enchelyomorpha vermicularis* (Smith, 1899) Kahl, 1930, an anaerobic ciliate (Protozoa, Ciliophora) from domestic sewage. *Acta Protozool.* **1995**, *34*, 21–34.
55. Rudzinska, M.A. The fine structure and function of the tentacle in *Tokophrya infusionum*. *J. Cell Biol.* **1965**, *25*, 459–477. [[CrossRef](#)]
56. Rudzinska, M.A. Do Suctorina really feed by suction? *Bioscience* **1973**, *23*, 87–94. [[CrossRef](#)]
57. Greening, C.; Ahmed, F.H.; Mohamed, A.E.; Lee, B.M.; Pandey, G.; Warden, A.C.; Scott, C.; Oakeshott, J.G.; Taylor, M.C.; Jackson, C.J. Physiology, biochemistry, and applications of F₄₂₀- and F₀- dependent redox reactions. *Microbiol. Mol. Biol. Rev.* **2016**, *80*, 451–493. [[CrossRef](#)]
58. Boxma, B.; de Graaf, R.M.; van der Staay, G.W.; van Alen, T.A.; Ricard, G.; Gabaldón, T.; van Hoek, A.H.; Moon-van der Staay, S.Y.; Koopman, W.J.; van Hellemond, J.J.; et al. An anaerobic mitochondrion that produces hydrogen. *Nature* **2015**, *434*, 74–79. [[CrossRef](#)] [[PubMed](#)]
59. Fenchel, T.; Finlay, B.J. The biology of free-living anaerobic ciliates. *Eur. J. Protistol.* **1991**, *26*, 201–215. [[CrossRef](#)] [[PubMed](#)]
60. Rotterová, J.; Salomaki, E.; Pánek, T.; Bourland, W.; Žihala, D.; Táborský, P.; Edgcomb, V.P.; Beinart, R.A.; Kolísko, M.; Čepička, I. Genomics of new ciliate lineages provides insight into the evolution of obligate anaerobiosis. *Cur. Biol.* **2020**, *30*, 2037–2050.e6. [[CrossRef](#)] [[PubMed](#)]
61. Kuever, J. The Family Syntrophaceae. In *The Prokaryotes*; Rosenberg, E., DeLong, E.F., Lory, S., Stackebrandt, E., Thompson, F., Eds.; Springer: Berlin/Heidelberg, Germany, 2014; pp. 281–288.
62. Bass, D.; Boenigk, J. Everything is everywhere: A twenty-first century reconstruction with respect to protists. In *Biogeography of Microscopic Organisms: Is Everything Small Everywhere?* Fontaneto, D., Ed.; Cambridge University Press: Cambridge, UK, 2011; pp. 88–110.
63. Fenchel, T.; Finlay, B.J.; Esteban, G.F. Cosmopolitan metapopulations? *Protist* **2019**, *170*, 314–318. [[CrossRef](#)]
64. Foissner, W. Protist diversity and distribution: Some basic considerations. *Biodivers. Conserv.* **2008**, *17*, 235–242. [[CrossRef](#)]
65. Agnarsson, I.; Kuntner, M. Taxonomy in a changing world: Seeking solutions for a science in crisis. *Syst. Biol.* **2007**, *56*, 531–539. [[CrossRef](#)]
66. Engel, M.S.; Ceriaco, L.M.; Daniel, G.M.; Dellapé, P.M.; Löbl, I.; Marinov, M.; Reis, R.E.; Young, M.T.; Dubois, A.; Agarwal, I.; et al. The taxonomic impediment: A shortage of taxonomists, not the lack of technical approaches. *Zool. J. Linn. Soc.* **2021**, *193*, 381–387. [[CrossRef](#)]
67. Acorn, J. Amateurs and abandoned science. *Am. Entomol.* **2009**, *55*, 127–128. [[CrossRef](#)]

68. Fischer, E.E.; Cobb, N.S.; Kawahara, A.Y.; Zaspel, J.M.; Cognato, A.I. Decline of amateur Lepidoptera collectors threatens the future of specimen-based research. *Bioscience* **2021**, *71*, 396–404. [[CrossRef](#)]
69. Gura, T. Citizen science: Amateur experts. *Nature* **2013**, *496*, 259–261. [[CrossRef](#)] [[PubMed](#)]
70. Bergerot, B. The Citizen Science Paradox. *Land* **2022**, *11*, 1151. [[CrossRef](#)]
71. Foissner, W.; Wenzel, F. Life and legacy of an outstanding ciliate taxonomist, Alfred Kahl (1877–1946), including a facsimile of his forgotten monograph from 1943. *Acta Protozool.* **2004**, *43*, 3–69.
72. Santaoja, M. Social media in learning on nature: Case Finnish amateur mycologists. *Horiz. Int. J. Learn. Futures* **2022**, *30*, 122–130. [[CrossRef](#)]

Disclaimer/Publisher’s Note: The statements, opinions and data contained in all publications are solely those of the individual author(s) and contributor(s) and not of MDPI and/or the editor(s). MDPI and/or the editor(s) disclaim responsibility for any injury to people or property resulting from any ideas, methods, instructions or products referred to in the content.